1968-03

An experimental investigation of the effects of environmental pressure on the exhaust of a coaxial plasma gun

Smith, Michael J.

Monterey, California. Naval Postgraduate School

AN EXPERIMENTAL INVESTIGATION OF THE EFFECTS OF ENVIRONMENTAL PRESSURE ON THE EXAUST OF A COAXIAL PLASMA GUN

MICHAEL J. SMITH

AN EXPERIMENTAL INVESTIGATION OF THE EFFECTS OF ENVIRONMENTAL PRESSURE ON THE EXHAUST OF A COAXIAL PLASMA GUN

by

Michael J. Smith
Ensign, United States Navy
B.S., U.S. Naval Academy, 1967

Submitted in partial fulfillment of the
requirements for the degree of

MASTER OF SCIENCE IN
AERONAUTICAL ENGINEERING

from the

NAVAL POSTGRADUATE SCHOOL
March 1968

ABSTRACT

A coaxial plasma accelerator system was restored to working order, and procedures for operating the system were established. Gold was used as the working material and was mounted as a thin circular foil between coaxial electrodes, ionized, and accelerated by discharging a high energy capacitor across the electrodes.

Downstream of the electrodes, part of the gold was collected on a cylindrical collector sheet of aluminum foil. This sheet surrounded the outer electrode and extended 16 inches above the muzzle. A radioisotope tracer technique was then used to determine the mass of deposited gold on sample disks cut from selected portions of the collector sheet. It was found that only a very small percentage of the total mass was collected and that the pressure effects, in the range from 5×10^{-5}mm Hg to 50×10^{-3}mm Hg, were such that an increase in exhaust pressure caused an increase in the mass of gold collected on the sheet; however, pressure effects on the distribution of this mass were negligible.

Thesis by Michael J. Smith entitled: "An Experimental Investigation of the Effects of Environmental Pressure on the Exhaust of a Coaxial Plasma Gun"

ERRATA SHEET

Page	Line	Change	To
19	21	solonoid	solenoid
21	23	oscilliscope	oscilloscope
22	17/18	fas-ter	fast-er
45	Fig. 1	PRESENSE	PRESENCE
82	Step 8	Appeindix	Appendix
86	Middle	Avagadro's	Avogadro's

TABLE OF CONTENTS

LIST OF TABLES

LIST OF ILLUSTRATIONS

ACKNOWLEDGEMENTS

The author wishes to express his appreciation to Professor D. C. Wooten of the Department of Aeronautics for his encouragement and assistance throughout the project and to Professors E. A. Milne and W. W. Hawes who made the Reactor Facility available and furnished technical aid with the tracer technique.

Appreciation also goes to Messrs. Theodore B. Dunton, Robert A. Besel, and Cecil R. Gordon who with the remainder of the technical staff of the Aeronautics Department furnished efficient technical help on the many electrical and mechanical problems encountered during the restoration of the system.

CHAPTER I

INTRODUCTION

The coaxial plasma accelerator built by R. E. Reichenbach and Lt. R. K. Brumwell has realized little experimental value to date because of the many problems encountered in obtaining proper operation of all components in the system. Data analysis techniques have been proposed but not thoroughly tested. Results of the tests have been inconclusive and have not established procedures which give repeatable results.

A. Brief History of Magnetohydrodynamics (MHD)

Introduced first as a method to solve astrophysical problems and problems associated with the fusion reactor, the field of MHD now treats problems in many different areas. Electrical space propulsion, hypersonic re-entry, and direct conversion into electrical energy of the thermal and kinetic energy in a flowing plasma require the study of the motion of intensely heated, ionized fluids and gases (11).

Since the presence of an electromagnetic field in which a conducting medium is moving induces currents in the medium and these currents in turn may change the electromagnetic field, one can see that this is quite a complicated problem. Here the electrical properties of the gases interact with their mechanical properties, which implies that the unification of two disciplines, gas dynamics and electromagnetics, is necessary to describe the phenomena. The resulting governing equations are Maxwell's equations coupled with the equations of fluid mechanics (7).

B. The Problem

In previous experiments (2) a thin gold foil was ionized and accelerated down the electrodes. These experiments were concerned with methods of determining the mass of gold plasma deposited on a collector cylinder and have produced some insight into the factors which influence the performance of the gun. In these experiments a radioisotope tracer technique was developed which allowed the determination of this unknown mass of gold. However, the ability of the system to perform repeatable experiments has never been established. Consistent functioning of the system as a whole was almost non-existent at the beginning of the experiment described in this thesis.

Many important and interesting experiments can be conducted using the plasma accelerator. Several of these are: 1) determining the impulse or thrust of the gun, 2) studying the effect of different shapes for the inner and outer electrodes, and 3) checking analytical models of the accelerator. Before these rather sophisticated experiments can be conducted, a knowledge of the effects of different parameters such as voltage, exhaust pressure, and electrode shape and their influence on the plasma will have to be obtained. This experiment was a step in this direction. Magnetohydrodynamics is a relatively new field with enormous potential for use in a variety of ways. A complete and thorough understanding of the plasma gun will give one a better grasp of this new subject and also advance the field.

It was the purpose of this experiment to: 1) restore the system to operation, 2) establish procedures which allow repeatable results, 3) establish the effect of exhaust pressure on the distribution of the mass of gold plasma which leaves the electrodes, and 4) perfect

the radioisotope tracer technique used to determine this distribution.

C. Definitions of Terms Used

Magnetohydrodynamics MHD. MHD is the study of the motion of conducting fluids and gases in an electromagnetic field.

Plasma. A plasma is highly ionized electrically conducting gas of neutral charge.

Lorentz Force. Lorentz Force is the force exerted on a current carrying object by a magnetic field. It is described by the equation:

$$\vec{F} = \vec{J} \times \vec{B} \qquad \text{(I-1)}$$

Hall Currents. Hall currents are currents which flow perpendicular to the E-field set up by a plasma with velocity v moving through an uniform B field. They produce a deflection or centripetal force $\vec{j}_h \times \vec{B}$ which produces a spiral trajectory for the plasma as v is reduced. This phenomenon is illustrated in Figure 1 (1).

CHAPTER II

DESCRIPTION OF EXPERIMENT

A. Accelerator Theory

Pulsed accelerators using electrodes operate in an unsteady fashion. The basic advantage of an unsteady device is that the thermal lag of the accelerator and the short time that the plasma is in contact with it combine to keep the material surface temperature low. This means that if pulsed accelerators are used, a plasma of very high energy or temperature can be created and handled without severe wall-erosion problems. Thus the efficiency can be kept high (12).

The basic mode of a pulsed accelerator with electrodes is shown in Figure 2a. When the switch is closed, the capacitor discharges, ionizing the working material. A strong (magnetic) B field is created, and the plasma is blown away from the electrodes by the Lorentz Force. However, since the plasma is relatively unconfined, the efficiency of this accelerator is low (12).

Confining the plasma to a T-tube geometry as shown in Figure 2b is one means of improving the efficiency. Although this geometry was conceived to give high velocities, it has achieved efficiencies of only 5 to 10 per cent when operated as a propulsive device (12).

Another method of achieving better efficiencies is the rail accelerator shown in Figure 3a. It should be noted that the rails help carry the current to the working material as it accelerates down the tube, which causes the Lorentz Force (propulsive force) to act on the plasma for a longer time. However, this apparent

improvement has actually yielded low efficiencies since the plasma is still relatively unconfined (12).

The coaxial accelerator used in this experiment and shown in Figure 3b is the logical combination of the two above approaches to achieve higher efficiencies. In this device the concentric electrodes provide the confinement and driving force. Experiments have shown that this combination does in fact give higher efficiencies. Specific impulses in the range of 5,000 to 25,000 seconds are possible with efficiencies on the order of 50 per cent compared with 1 per cent efficiencies for earlier devices. The coaxial arrangement successfully increases the coupling of the capacitor energy to the plasma and prevents the increase in plasma resistance as the plasma accelerates (12).

Although the basic principles underlying the design of the coaxial plasma accelerator have been studied to some extent, most experimental apparatus are the result of expediency. This is because the complex interactions involved in an experimental device of this type are not yet fully understood. Many studies to determine these complex interactions have been performed; nevertheless, there is still relatively little information available on the operation of a coaxial plasma gun. However, there are several experiments which give one a better insight into the problem; these are described below.

Keck (5) observed that when the ratio of the outer to inner radius is large (>2), the speed, shape, and thickness of the plasma or "current sheet" in the coaxial accelerator unexpectedly depend upon the polarity of the electrodes. When the center electrode is

positive, the average speed is higher than when the center electrode is negative. For a negative (inward) radial electron current which occurs with positive polarity of the center electrode, the current sheet was found to be more than twice as thick as when the polarity was reversed. Also a negative polarity gives a current sheet which is almost perpendicular to the walls while the opposite polarity causes a bullet-shaped plasma. The bullet-shaped plasma would be the most likely shape since the magnetic pressure varies as $1/r^2$ (1). The center electrode of the coaxial accelerator used in the present experiment was of negative polarity.

These phenomena were investigated by Fishman and Petschek (3) who suggested that the difference in operation between positive and negative polarity is associated with the problem of electron emission at the electrodes. They hypothesized that there is insufficient electron emission from the electrodes and that this tends to force the flow towards a configuration (planar or bullet-shaped) which allows the current to be carried by the ions.

W. A. Bostick (1) partially explained the shape of the current sheet and its dependence upon the polarity of the electrodes by a combination of hall currents and plasma vortices, both of which are expected to occur in such an accelerator.

There are two major models used to describe the plasma accelerator. The "snowplow" model assumes that in the absence of external electric or magnetic fields the current is axially symmetric and flows radially from one coaxial electrode to the other as a thin disk. This disk contains all the mass "scooped up" as it moves outward a distance x measured from the insulation at the base of the

electrodes as shown in Figure 4a. This model is used when the plasma is being accelerated into a region having an uniform gas distribution. The second model shown in Figure 4b is the "slug" model used to describe the motion of a constant mass of plasma which is accelerated into a vacuum (4) .

The results of experiments have raised the following unanswered questions: 1) How does the large current pass from the electrodes into the plasma without detaching major quantities of electrode material as ions, especially at the anode (11)? 2) How do the J x B mechanisms vary in different regions due to current loops? 3) In the model proposed in reference (3) there is implied a radial mass flow which would allow ions to carry current when the center electrode is positive, making electron emission at the cathode unnecessary. When the center electrode is negative, the ion flow opposes the electron current. Does a mode of operation develop in which the mass flow is radially inward to provide appropriate ion current in the absence of sufficient electron emission at the cathode?

Further analytical and experimental work on the processes which occur in the current sheet itself is necessary before the current sheet and the coaxial accelerator can be fully understood. The effort described in this thesis is experimental in nature, and a description of the system follows.

B. The Accelerator

The coaxial configuration used for the electrodes of the accelerator is shown in Figure 5. The electrodes are in a vertical position directly over the ignitrons and capacitor. The electrodes come apart at the foil plane to allow loading. The disassembled electrodes

with a gold foil nearby are shown in Figure 6. After the foil was laid in place at the foil plane, the 1-inch O.D. inner electrode was screwed down to hold the foil in place. The 1.5-inch I.D. outer electrode was then placed over the foil with the barrel acting as a nonrotating washer held in place by a lipped, screw-down flange as shown in Figure 5. Because of an alignment error the electrodes were not perfectly concentric. The axes of the two electrodes were approximately 1/32 inch apart at the top. In order to keep this misalignment the same for all shots, scribe marks were employed on the electrodes to insure that they were replaced the same each time. Gold was used as the working material because of its availability in thin sheets, purity in commercial form, convenient radioactive half-life (2.7 days) and large activation cross section (98.8 barns) (2) . The gold was in the form of foils 0.0005 inches thick weighing 19.25 milligrams.

C. Capacitor System

Discharge circuit. To ionize the gold foil, an Axel Co. 6.4 microfarad low inductance capacitor with a 2000 joule capacity at 25,000 volts was discharged across the electrodes. Two GE 7703 ignitrons in parallel provided the switching. These ignitrons were rated at 20 KV and 100,000 amps peak current. The capacitor case was connected by heavy brass bars to the aluminum base which supported the electrodes, and this entire unit was grounded. The ignitrons floated electrically at capacitor potential. Figure 7 shows the installation of the ignitrons and capacitor. There were originally four ignitrons used in the circuit; however, two were not working at the time of the experiment. As a safety measure, a grounding rod with a phenolic handle was connected to the capacitor when it was not in use.

Ignitron triggering circuits. The ignitrons were triggered by the pulser circuit shown in Figure 8. The 6268 thyratron in the circuit is used to provide a 3000 volt pulse with a rise time of about 0.5 microseconds necessary to trigger the ignitrons. The pulse transformer located between the pulser circuit and the ignitrons is shown in the bottom of Figure 9b. It isolates the ignitrons from the pulser circuit and inverts the pulse.

The pulser circuit is triggered by the circuit shown in Figures 10 and 11a. This circuit employes a 2021 thyratron to give a 120 volt pulse with a rise time of 0.15 microseconds to trigger the thyratron in the pulser circuit.

Charging circuit. A 40 KV power supply was used to charge the capacitor. This circuit is shown in Figure 12, and the high voltage controls are shown in Figure 11b. A normally closed Jennings high-voltage relay was connected in parallel with the power supply main switch. In the event that a shot had to be aborted, the main switch was opened which shut down the power supply and also grounded the capacitor through a 1 megohm high-voltage resistor which dissipated the power. This resistor also bled residual capacitor energy to ground after firing (2).

Charging was accomplished through a solonid operated knife switch and a 3 megohm high-voltage resistor. The charging (top) and abort (bottom) resistors and Jennings relay are shown in Figure 13. In order to read capacitor potential directly, a microammeter in series with a 600 megohm resistor was connected across the capacitor (2).

D. Vacuum System

The vacuum system shown in Figure 14 consisted of two main parts.

It was used to evacuate a 14-inch bell jar which encloses the electrodes. Since removing the collector sheet and reloading the gun required removal of the bell jar, the dual vacuum system was required to provide rapid evacuation after the reloading process.

A Welch 13978 pump (Figure 15b) was used to initially "rough" the system down to a pressure of about 10^{-3} millimeters of mercury. The high vacuum system, shown in Figure 15a, consisting of a 4-inch Veeco combination diffusion pump, baffle, and nitrogen cold trap and a Welch 14208 fore pump then reduced the system to the desired pressure. A log log plot of pressure versus time is shown in Figure 16a and gives an indication of the time required to pump down to a pressure between 2×10^{-4} mm Hg and 6×10^{-5} mm Hg using the high vacuum system. Deviation from the curve during pump down would indicate a leak. Pressures of 5×10^{-5} mm Hg were obtained using this system without the nitrogen cold trap.

Connections from the roughing pump and diffusion pump to the heavy aluminum manifold which supported the bell jar were made through 1.5-inch I.D. pipe. Flange type joints were used with O-ring seals. This assembly is shown in Figure 5. Two-inch Stokes gate valves were used to connect or disconnect the roughing pump or diffusion pump to the system. As shown in Figure 14 these are valves 1 and 4. Veeco 3/4-inch vacuum valves were used in positions 3 and 5. Valve 5 was used to bleed air into the diffusion pump exhaust and fore pump inlet. This was necessary because if the fore pump is shut down, the large pressure difference between the two pumps causes fore pump oil to be drawn into the diffusion pump. Valve 3 allowed ionization gauge 1 to be connected to the bell jar. Valve 2, used to bleed air into the

bell jar, was a standard gate valve.

A water flow switch incorporated into the diffusion pump coolant water line automatically shut off the diffusion pump in the event of a water flow failure. The switch is shown in Figure 16b and is located in the vacuum control circuit as shown in Figure 17. This control circuit also protected the diffusion pump against fore pump failure (operation at pressures above 500 microns) and required a manual reset after either a coolant water or fore pump failure.

E. Instrumentation

Vacuum measurement was by Veeco DV1M thermocouple gauges and RGK-75 ionization gauges controlled through a Veeco control panel shown in Figure 9a. The thermocouple gauges were placed in the system as shown in Figure 14 and measured pressures down to 1 micron (10^{-3}mm Hg). It should be noted that these gauges had to be calibrated often in order to give reliable readings. At pressures below 1 micron the more accurate ionization gauges were used. After calibration this system proved reasonably accurate and very easy to use.

Discharge monitoring of the electrode current was accomplished by observing a CRT display of the current versus time during capacitor discharge. This was done by using a single loop of wire under the aluminum electrode base to pick up the induced current pulse. A 10:1 probe in series with a 20 megohm resistor was used to attenuate the signal to the memory oscilliscope.

An image converter camera was available to photograph the plasma; however, it remained out of order during the time the experiments were conducted. Three loops of test lead wire wrapped around the pulse transformer box are sufficient to pick up an induced pulse with the required characteristics to trigger the camera.

F. Firing Procedure

The firing procedure was developed using previous procedures given in reference (2) and adding to or eliminating steps as necessary to improve reliability of successive shots.

First the roughing pump and fore pump were started. Residual gold foil from the previous shot deposited at the base of the electrodes was removed by a vacuum cleaner. A collector sheet was then positioned in the collector tube using the ends of the spacers located on the tube to line it up and insure that it was in the same position for each shot. The sheet was held in place by small spring steel clamps located at the ends of the sheet. All components inside, including the bell jar, were cleaned using acetone. The gold foil was carefully placed in position and the electrodes screwed into place with care being taken to insure line-up of the scribe marks. After the collector tube was in place, the inside of the bell jar and surfaces under the bell jar were heated with a heat gun to partially evaporate moisture and cleaning fluid and to facilitate faster pump-down. Figure 18 shows the coaxial gun loaded and ready for the bell jar to be lowered. After the bell jar was lowered, the vacuum system was connected to the system as described in Appendix A. When the desired pressure was reached, the firing procedure described in Appendix B was followed. After the shot the collector sheet was processed as described in Section B, Chapter III, on Tracer Technique.

CHAPTER III

RADIOISOTOPE TRACING TECHNIQUE

A radioisotope tracer technique was used to determine the amount of gold deposited at selected stations along the collector sheet.

A. Tracer Theory

The capture of neutrons by certain materials when exposed to neutron flux produces radioactive nuclides. The activity of these isotopes provides a way to determine the amount of radioactive material present by comparing it with a known amount of the same material which has been exposed to the same amount of flux (9).

The induced radioactivity in an irradiated source (that is, one which has been exposed to an amount of neutron flux) decreases as time passes. This decay or rate of decrease is exponential and varies with the individual isotope. We can express the decay mathematically by the equation:

$$A_t = A_o \left(e^{\frac{-0.693\, t}{T_{\frac{1}{2}}}} \right) = A_o e^{-\lambda t} \qquad \text{(III-1)}$$

where A_o = initial activity (disintegrations per unit time)

A_t = activity remaining after time t

$T_{\frac{1}{2}}$ = half-life (period of time taken for the activity to decrease by one-half), expressed in convenient units

t = elapsed time, in same units as $T_{\frac{1}{2}}$.

It should be noted that Equation (III-1) is statistical in nature and does not hold for very low activities (9).

The induced activity in a sample is dependent on: 1) the amount of the target element present, 2) the cross section of the nuclide, 3) the irradiation flux, 4) the irradiation time, and 5) the decay

characteristics of the element formed. All of these factors which influence the final activity of a sample due to activation of a given nuclide can be expressed in the following equations:

$$A = N\sigma\phi\left(1 - e^{-\lambda t_e}\right) \qquad \text{(III-2)}$$

But since

$$\lambda = \frac{0.693}{T_{1/2}} \qquad \text{(III-3)}$$

Upon substitution of equation (III-3) into (III-2) we obtain:

$$A = N\sigma\phi\left[1 - \exp\left(-\frac{0.693\, t_e}{T_{1/2}}\right)\right] \qquad \text{(III-4)}$$

where A = induced activity present at end of irradiation, dis/sec

N = number of target atoms

σ = cross section, cm^2

ϕ = irradiation flux, neutrons/cm^2/sec

t_e = irradiation time

$T_{1/2}$ = half-life of product nuclide

λ = decay constant of product nuclide

Equation (III-4) is known as the activation equation (9) .

There are two methods in use to determine unknown mass of elements which have been activated. The first is an absolute determination using the activation equation. It requires that σ , ϕ , t_e, and $T_{1/2}$ be known and that A be determined experimentally. However, there are three basic faults associated with this method which make it undesirable. They are: 1) The cross sections of most nuclides are probably known to no better than between 5 and 10 per cent, 2) the flux can vary during irradiation, or flux gradients can exist in the sample, or the flux is simply not accurately known, and 3) it is

difficult and time consuming to make absolute activity measurements on the sample (9).

The other method is known as the comparator method and is the one used in this experiment. In this method a pure sample of known mass of the sought element and the unknown (mass) sample are irradiated together for the same time and in the same flux. Since, under ideal conditions the specific activities (disintegration rate/mass of sample) are the same for the known and unknown samples one may simply count the known and unknown samples under identical conditions and use the relationship (9):

$$\text{unknown mass} = \left[\frac{\text{activity of unknown mass}}{\text{activity of known mass}}\right] (\text{known mass}) \qquad \text{(III-5)}$$

to determine the unknown mass. Equation (III-5) is developed in Appendix C.

In this experiment gold 197 was irradiated in the small AGN201 research reactor in building 223 at the Naval Postgraduate School. Gold undergoes the reaction:

$$n + Au^{197} \rightarrow Au^{198*} + \gamma \qquad \text{(III-6)}$$

where the neutron interacting with the gold atom produces an excited (*) residual nucleus which decays, emitting gamma (γ) rays.

These gamma rays are counted by a scintillation counter which makes use of the luminescence of the inorganic solid NaI(Tl) and a photomultiplier tube to detect and count the gamma rays. As a gamma photon interacts with the NaI(Tl) crystal, the result is the production of high energy electrons which are responsible for the luminescence. The photomultiplier tube picks up this luminescence in the

form of photons and changes them to voltage pulses. These voltage pulses are fed into an electronic amplifier which boosts them to a level that will trigger a scaling circuit. Here pulse height analyzing equipment takes over and gives the gamma ray spectrum (9).

B. Tracer Technique

When the gold foil is ionized and accelerated from the electrodes, it has been shown in previous experiments (2) that downstream of the exhaust of the electrodes a certain amount of gold diffuses outward in a radial direction and is deposited on the sides of the collector cylinder. In order to pick up this gold and use the tracer technique, common household aluminum foil was used as the material for the collector sheet because aluminum has a low background activity. The activities of three different Al control disks are plotted versus time after irradiation in Figure 19. The disks all received the same amount of flux; therefore, we can use the activities of all three to plot the curve shown. It should be noted that this curve is not the familiar exponential decay curve which obeys equation (III-1). This is because the foil contains impurities all of which have different half-lives or decay constants.

The collector sheet was 4.56 inches wide and 18 inches high. It extended 16 inches above the muzzle and was held close to the sides of the 2.4-inch I.D. collector tube by 1/8-inch spring steel clips. After the shot the collector sheet was removed from the supporting tube and sprayed with lacquer to keep the deposited gold from shifting accidentally. Sample disks 0.73 inches in diameter were cut at selected intervals on the collector sheet as shown in Figure 20. Each sample was given an identifying number such as:

[number 1] [I or O] [L or R]-[number 2]

where

number 1 = shot number

I = inside of collector sheet (for an inside sample the distance from the lengthwise edge of the collector sheet to the center of the sample disk was 1.69 in.)

O = outside of collector sheet (distance from lengthwise edge of collector sheet to center of sample disk was 0.56 in.)

L = left side of collector sheet

R = right side of collector sheet

number 2 = distance in inches from the muzzle of the accelerator.

An example number would be:

40L-9.

The samples were then prepared for irradiation by placing them in a tube-like holder shown in Figure 21b. Figure 21a shows the distribution and variation of flux at core center. During irradiation the center of the 1-inch spacer separating the two groups of samples was placed at core center to insure that both groups received the same amount of flux. The fact that they did receive the same flux is discussed further in Section A of Chapter IV. The group of sample disks from shot 5 was irradiated at 100 watts for a time of 10 minutes while all successive shots were irradiated at 300 watts for 10 minutes in order to induce sufficient activity to give reasonable accuracy when counting. The error in counting can be shown to be equal to the square root of the number of counts per unit counting time (9).

After irradiation the samples were allowed to sit for 24 hours

to allow the radioactive elements in the aluminum foil to decay to a value of about 84 counts per minute as shown in Figure 19. Since the half-life for gold is much longer than that for the foil, the gold counts were not reduced appreciably.

The activities of the sample disk and control disks were then determined by using a scintillation counter and a multichannel pulse height analyzer. The scintillation counter consisted of a 3 x 3-inch Harshaw well crystal integrally mounted on a photomultiplier tube. The output of the photomultiplier tube directly drives a nuclear data ND180 system. The entire detection and analyzing system is shown schematically in Figure 22. The counting procedure and ND180 operation is given in Appendix D.

To determine the activity of the sample disks and control sample only the number of counts in the 16 channels to the left and right of the 0.411 Mev peak were used. This saved time and did not affect the accuracy of the measurement. Since, to determine the unknown mass of gold, we are using the ratio of the activities, which means that as long as we count the control samples and sample disks over the same energy or channel range, the ratio should be the same. Each sample disk was placed in a small plastic box to insure that the same geometry was presented each time; then the disk was counted for 10 minutes. Figure 23 shows the number of counts versus energy level or channel for the 16 channels to the left and right of the 0.411 Mev peak during a 10-minute count of a typical sample. After the ND180 had printed out the number of counts per channel for the sample being counted, the selected channels surrounding the 0.411 Mev peak were summed. Equation (III-5) was then used to determine the unknown mass

on the sample disk. See Appendix E for the description of the preparation of Al and Au control samples.

CHAPTER IV

RESULTS AND CONCLUSIONS

A. Results and Discussions

Accelerator system. The accelerator system functions properly with only two ignitrons in operation; however, charging the capacitor above 10 KV is prohibited by one of the faulty ignitrons because voltages in excess of this cause a breakdown, discharging the capacitor. Discharge monitoring is not yet complete because of the absence of the image converter camera.

Tracer analysis. Since the basic tracer analysis technique had already been established (2), initial tests (shots 4 and 5) were run under the suggested irradiation conditions of 100 watts for 10 minutes. The foils were arranged in the holder as shown in Figure 24a. The results of shot 5 in Table I indicate that enough activity was not induced to give a reasonably accurate count over a 10-minute counting time. It was necessary to count these samples for a period of 40 minutes to obtain accuracies of about 2 to 3 per cent. Shot 4, although irradiated, was not counted because of the long counting times involved and the extended period of time since irradiation (10 days).

For shot 6 the foils were arranged in the holder as before; however, the irradiation conditions were changed to 300 watts for 10 minutes. The results shown in Table II show that the increased power during irradiation allowed a substantial decrease in counting time while increasing the overall counting accuracy to about 1 per cent. The two gold control samples in the center of each group of samples were monitored throughout the counting time to insure that both groups were receiving the same amount of flux. From equation (C-12) it is

evident that if the two control samples receive the same flux, then the ratios of their masses should be equal to the ratios of their activities at some time after irradiation. The fact that the flux received by both samples is the same is shown in Figure 24b.

One more irradiation was made. The holder contained selected samples from shots 7, 8, 12, 13, and 14 arranged as shown in Figure 25. The irradiation conditions were the same as those for shot 6.

Portions of shots 7, 8, 12, 13, and 14 were analyzed and the results are shown in Tables III - VII and Figures 26 - 30. Shots 6 and 7 were used as check on the repeatability of the system while the results of all shots except 5 were used to determine the effect of exhaust pressure on the mass distribution leaving the electrodes. The mass distribution for shots 5 and 6 are shown in Figures 31 and 32 respectively.

The 3 per cent difference in mass deposited within the collecting cylinder for shots 6 and 7 indicates that the flow was neither axially symmetric for either shot nor the same for either shot even though the firing conditions were identical. The respective figures for shots 5, 7, 8, and 12 through 14 also indicate that the mass distribution is not axially symmetric.

A plot of percentage of total mass deposited within 10 inches of the collector tube versus pressure (Figure 33a) shows that there is a slight trend for more mass to be deposited on the collector sheet as pressure is increased above 10^{-4} mm Hg.

For shots 12, 13, and 14 a collector whose configuration is shown in Figure 33b was placed over the top of the collector tube to determine the amount of gold that was leaving the open end. These results

are presented in Table VIII and Figure 34. Also an estimate of the percentage of gold deposited in the 16 inches of the collector tube above the muzzle was made, and the results are shown in Figure 34. The sums of the percentages for mass deposited on the sides and mass leaving the top for shots 12, 13, and 14 are also shown in Figure 34. Figure 35 shows the average mass distribution for shots 6, 7, 8, 12, 13, and 14. This average was computed by obtaining an average distribution around the cylinder for each 2-inch segment of the collector sheet from samples taken from applicable areas. It should be noted that the peak of the average mass distribution occurs at approximately 5 inches from the muzzle for each shot and that the variation in mass distribution is not large except for shot 6.

B. Explanation of Results

The fact that the mass distribution in the angular direction is not constant could be explained by the fact that the electrodes do not exert an even clamping pressure on the gold foil nor are their surfaces smooth enough to insure a good electrical contact. With the high voltages involved, these discrepancies could cause or aid the arc discharge to form a spoke rather than an axially symmetric current flow from one electrode to the other. One or more spokes in the plasma could explain the departure from axial symmetry as well as the peaks in mass distribution at different angular positions shown in Figures 32 and 31 for shots 5 and 6 respectively.

A rough estimate of the effect of pressure on the mass distribution in the ranges from 5×10^{-5} mm Hg to 50×10^{-3} mm Hg indicates that pressure had some effect as described in Section B, Chapter IV and Figure 33a. The somewhat erratic curve of percentage of mass

deposited versus pressure (Figure 33a) can be considered a consequence of inefficient and uneven ionization of the gold foil.

The low percentage of mass collected is thought to be the result of nonuniform or spoke discharge. After each shot relatively large portions of the gold foil were observed at the base of the electrodes, and smaller particles were found scattered around the outside of the electrodes indicating that only part of the foil was ionized while the remainder tore into particles of varying sizes. Hence, some of these particles are never accelerated while the ones that are could be discharged as small globs and never be collected.

C. Conclusions

The accelerator works but at the present time functions very inefficiently. Operating procedures have been established which allow safe and reliable operation of the system. Parts of the original tracer technique were found to be insufficient to give accurate results and were modified accordingly. It was found that if sample disks are placed in the holder tube so that the samples were not spread over a distance greater than 3 inches and that if the center of this 3-inch distance were placed at the reactor core center, all samples would receive the same amount of flux. The vacuum system is capable of producing a vacuum of the order of 10^{-5} mm Hg without use of the cold trap.

The mass distribution is not axially symmetric. There was a slight decrease in total mass collected with increasing pressures for shots 12, 13, and 14. However, it should be emphasized that these results are based on an estimated gold deposit in the last 6 inches of the collector sheet. Although slight, there does appear

to be a direct relation between the mass deposited on the collector cylinder and an inverse relation between pressure and the mass exhausted out of the top of the collector cylinder. The position of the peak average mass distribution does not seem to be affected by the exhaust pressure.

D. Suggestions for Further Investigation

A large number of interesting and informative experiments could be performed using the plasma gun described in this report after a few corrections are made to the system. These corrections are:

1) Making a new set of electrodes that are coaxial.
2) Installing new or rebuilt ignitrons.
3) Repairing the image converter camera.
4) Designing a better way of mounting the collector sheet inside of the collector cylinder so that a closer and smoother fit can be established between the sheet and cylinder walls.

E. Suggestions for Further Experimentation

1) Determining the mass distribution obtained from ionizing one-half of a gold foil.
2) Determining the specific impulse of the gun.
3) Calculating the efficiency of the system.
4) Mounting a camera directly over the electrodes to determine what takes place at the foil plane when the capacitor is discharged.
5) Establishing the characteristics of the gun by conducting a parametric study.

BIBLIOGRAPHY

1. Bostick, W. H. "Hall Currents and Vortices in the Coaxial Plasma Accelerator," The Physics of Fluids, 6, pp. 1598-1603, Nov., 1963.

2. Brumwell, R. K. Radioisotope Tracing of Metallic Deposits Near a Coaxial Plasma Gun Exhaust, A. E. Thesis, Naval Postgraduate School, 1966.

3. Fishman, F. J. and H. Petschek. "Flow Model for Large Radius-Ratio Magnetic Annular Shock Tube Operation," The Physics of Fluids, 5, pp. 632-3, May, 1962.

4. Hart, P. J. Plasma Acceleration with Coaxial Electrodes, Lockheed Aircraft Corporation, 1961.

5. Keck, James C. "Current Distribution in a Magnetic Annular Shock Tube," The Physics of Fluids, 5, pp. 630-2, May, 1962.

6. King, G. C. D. Nuclear Power Systems, New York: MacMillan Co., 1964.

7. Kulikovsiy, G. and Lyubimov, G. Magnetohydrodynamics, Reading: Addison-Wesley Publishing Co., Inc., 1965.

8. Landshoff, Rolf K. M. (ed.) Magnetohydrodynamics, Stanford: Stanford University Press, 1957.

9. Lyon, William S. Jr. (ed.) Guide to Activation Analysis, Princeton: D. Van Nostrand Co., Inc., 1964.

10. Marshall, J. "Performance of a Hydromagnetic Plasma Gun," The Physics of Fluids, 3, pp. 134-5, Feb., 1960.

11. Pai, Shih-I. Magnetohydrodynamics and Plasma Physics, Englewood Cliffs: Prentice-Hall, Inc., 1962.

12. Sutton, W. and Sherman, A. Engineering Magnetohydrodynamics, New York: McGraw-Hill Book Co., 1965.

TABLE I

TRACER RESULTS FOR SHOT 5 (40 minute counting time)

SAMPLE	ACTIVATED	AGE Hrs.	ACTIVITY Counts/min	CONTROL ACTIVITY Counts/min	CONTROL MASS milligrams	AGE Hrs.	BACKGROUND Counts/min	DEPOSITED MASS μgms/in.^{2}
50L-0		174.33	70					3.28
2		172.61	75					4.25
4		171.63	95	95,000	6.47	150.3	54	8.11
6		170.66	130					14.90
8		169.78	88					1.38
10		167.83	46					0.00
5IL-0		174.75	58					0.66
2		153.45	80					4.31
4		152.65	80					4.20
6		151.92	83					4.70
8		151.02	68					2.10
10	30 January	151.00	48					0.00
5IR-0	1968	221.73	66					5.80
2	1505	221.02	77					2.69
4		200.74	85					7.13
6		199.90	111					16.48
8		199.19	60					2.41
10		198.40	48					0.00
50R-0		197.40	72					5.57
2		196.65	73					5.83
4		194.98	82					8.00
6		194.06	86					9.04
8		192.41	89					10.04
10		191.41	52					0.00

TABLE II

TRACER RESULTS FOR SHOT 6 (10 minute counting time)

SAMPLE	ACTIVATED	AGE Hrs.	ACTIVITY Counts/min	CONTROL ACTIVITY Counts/min	CONTROL MASS milligrams	AGE Hrs.	BACKGROUND Counts/min	DEPOSITED MASS μgms/in.^{2}
60L-1		13.60	109					0.00
2		13.45	230					0.07
3		13.25	507					3.25
4		13.00	998					11.11
5		12.70	1266	42768	0.25	10.62	225	14.90
6		12.50	1643					20.26
7		12.07	1530					18.57
8		4.95	1453					16.19
9		11.92	1199					13.82
10	16 February 1968 1030	11.50	915					9.75
6IL-1		39.13	68					0.00
2		38.91	132					1.50
3		38.66	395					8.35
4		38.25	1290					36.61
5		37.75	1743	26355	0.30	42.58	75	43.19
6		37.50	1472					36.12
7		37.08	1636					40.12
8		36.83	1390					33.70
9		36.58	1132					27.05
10		15.58	581					10.28

TABLE II (continued)

SAMPLE	ACTIVATED	AGE Hrs.	ACTIVITY Counts/min	CONTROL ACTIVITY Counts/min	CONTROL MASS milligram	AGE Hrs.	BACKGROUND Counts/min	DEPOSITED MASS μgms/in.^{2}
6IR-1		41.83	145					0.00
2		41.58	194					3.20
3		41.25	1256					31.72
4		41.00	1817					46.70
5		40.75	4387	26355	0.30	42.58	75	115.63
6		40.50	2323					60.12
7		40.04	1380					34.61
8		39.79	1897					41.19
9		39.63	2040					51.90
10	16 February 1968 1030	39.38	444					9.72
60R-1		55.25	65					0.00
2		55.00	199					2.80
3		54.75	452					8.30
4		54.50	1148					23.10
5		54.25	830	27394	0.25	55.83	70	16.30
6		54.00	970					19.20
7		53.75	1655					33.80
8		53.50	1063					21.10
9		53.25	607					11.42
10		53.00	1122					22.30

TABLE III

TRACER RESULTS FOR SHOT 7 (10 minute counting time)

SAMPLE	ACTIVATED	AGE Hrs.	ACTIVITY Counts/min	CONTROL ACTIVITY Counts/min	CONTROL MASS milligrams	AGE Hrs.	BACKGROUND Counts/min	DEPOSITED MASS μgms/in.^{2}
7OL-1	21 February 1968 1119	26.91	242	17453	0.18	25.16	85	8.50
2		26.66	383					7.49
4		26.41	948					21.55
6		26.16	886					19.94
9		25.91	660					14.27
10		25.66	484					9.72
7IL-1		29.41	149	17453	0.18	25.16	85	1.67
2		29.16	289					5.24
4		28.16	896					20.60
6		27.66	766					17.24
8		27.41	430					8.71
10		27.16	454					9.30
7IR-1		31.41	375	16489	0.18	29.66	78	7.94
2		31.16	232					4.10
4		30.91	763					18.19
6		30.66	828					19.87
8		30.41	747					18.49
10		30.16	703					16.47
7OR-1		32.89	148	16489	0.18	29.66	78	1.92
2		32.61	369					7.87
4		32.33	891					21.94
6		32.16	1161					29.17
8		31.91	746					17.93
10		31.66	531					12.14

TABLE IV

TRACER RESULTS FOR SHOT 8 (10 minute counting time)

SAMPLE	ACTIVATED	AGE Hrs.	ACTIVITY Counts/min	CONTROL ACTIVITY Counts/min	CONTROL MASS milligrams	AGE Hrs.	BACKGROUND Counts/min	DEPOSITED MASS μgms/in.^{2}
80L-1	21 February 1968 1119	57.25	85	11829	0.18	55.16	66	0.44
2		57.00	102					1.18
4		56.75	733					24.80
6		56.50	822					28.09
8		56.25	499					16.07
10		56.08	438					13.76
80R-1		57.25	85	11829	0.18	55.16	66	0.44
2		58.42	87					0.78
4		58.17	253					7.09
6		57.92	151					3.22
8		57.75	409					12.90
10		57.50	322					9.59

TABLE V

TRACER RESULTS FOR SHOT 12 (10 minute counting time)

SAMPLE	ACTIVATED	AGE Hrs.	ACTIVITY Counts/min	CONTROL ACTIVITY Counts/min	CONTROL MASS milligrams	AGE Hrs.	BACKGROUND Counts/min	DEPOSITED MASS μgms/in.^{2}
120L-0		60.41	71					0.28
2		60.16	217					6.09
4		59.91	580	11395	0.18	58.66	59	19.98
6		59.74	406					13.28
8		59.57	388					12.59
10	21 February 1968 1119	59.33	638					22.08
120R-0		60.41	71					0.28
2		61.58	166					4.17
4		61.33	289	11395	0.18	58.66	59	8.95
6		61.08	352					11.37
8		60.83	435					7.61
10		60.58	348					11.18

TABLE VI

TRACER RESULTS FOR SHOT 13 (10 minute counting time)

SAMPLE	ACTIVATED	AGE Hrs.	ACTIVITY Counts/min	CONTROL ACTIVITY Counts/min	CONTROL MASS milligrams	AGE Hrs.	BACKGROUND Counts/min	DEPOSITED MASS μgms/in.^{2}
130L-0	21 February 1968 1119	49.41	172	13227	0.18	49.91	65	8.49
2		49.16	294					7.40
4		46.16	965					28.02
6		45.91	546					18.06
8		45.66	466					12.41
10		39.07	288					6.47
130R-0		54.99	81	13227	0.18	49.91	65	0.69
2		54.74	225					5.45
4		54.49	604					18.31
6		54.24	485					14.22
8		53.99	483					14.14
10		50.98	506					14.40

TABLE VII

TRACER RESULTS FOR SHOT 14 (10 minute counting time)

SAMPLE	ACTIVATED	AGE Hrs.	ACTIVITY Counts/min	CONTROL ACTIVITY Counts/min	CONTROL MASS milligrams	AGE Hrs.	BACKGROUND Counts/min	DEPOSITED MASS μgms/in.^{2}
140L-0		35.57	118					1.18
2		35.32	458					10.53
4		35.15	787					19.51
6		34.98	882	16133	0.18	33.06	75	22.08
8	21	34.73	443					10.00
10	February 1968	34.56	686					16.61
140R-0	1119	37.32	158					1.20
2		37.07	499					11.88
4		36.82	879	16133	0.18	33.06	75	22.43
6		36.57	481					11.35
8		36.32	630					17.10
10		36.07	969					24.76

TABLE VIII

TRACER RESULTS FOR MASS COLLECTED AT THE TOP OF COLLECTOR

CYLINDER FOR SHOTS 12, 13, 14 (10 minute counting time)

SAMPLE	ACTIVATED	AGE Hrs.	ACTIVITY Counts/min	CONTROL ACTIVITY Counts/min	CONTROL MASS milligrams	AGE Hrs.	BACKGROUND Counts/min	DEPOSITED MASS μgms/in.^{2}
12T	21 February 1968 1119	69.08	3976	11395	0.18	58.66	59	69.70
12T		69.33	3443					60.20
12T		69.58	3731					65.85
12T		69.83	5942					105.13
12T		70.38	6246					111.10
13T		39.32	4595	13371	0.18	49.90	65	52.44
13T		39.57	4971					57.12
13T		39.83	9785					115.21
13T		44.97	5788					71.58
13T		45.41	3919					50.50
14T		37.82	1301	16133	0.18	33.06	75	14.40
14T		38.07	3531					40.82
14T		38.32	6348					74.35
14T		38.57	2289					26.33
14T		37.57	3289					37.74

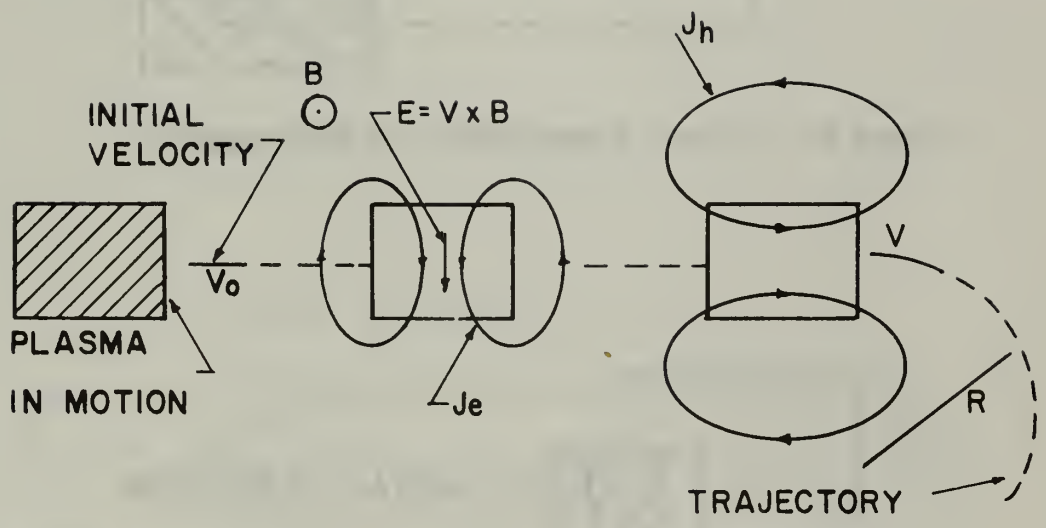

Figure 1. EXAMPLE OF LORENTZ CURRENTS Je AND HALL CURRENTS J_h WHICH FLOW IN A MORSEL OF PLASMA WHICH IS IN MOTION ACROSS A MAGNETIC FIELD IN THE PRESENSE OF A CONDUCTING MEDIUM

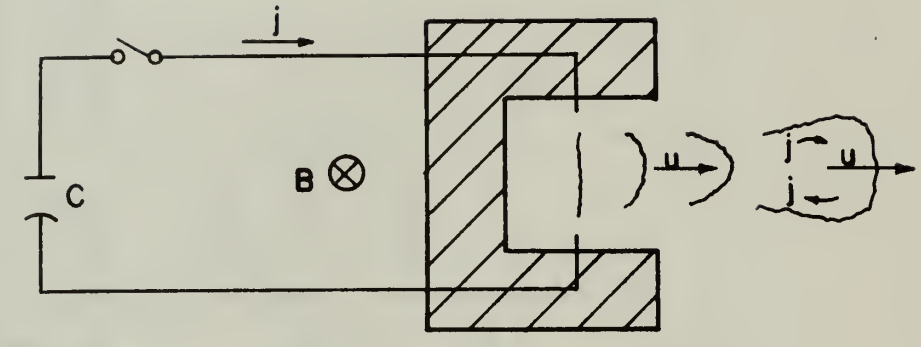

Figure 2a. Pulsed Accelerator with Electrodes

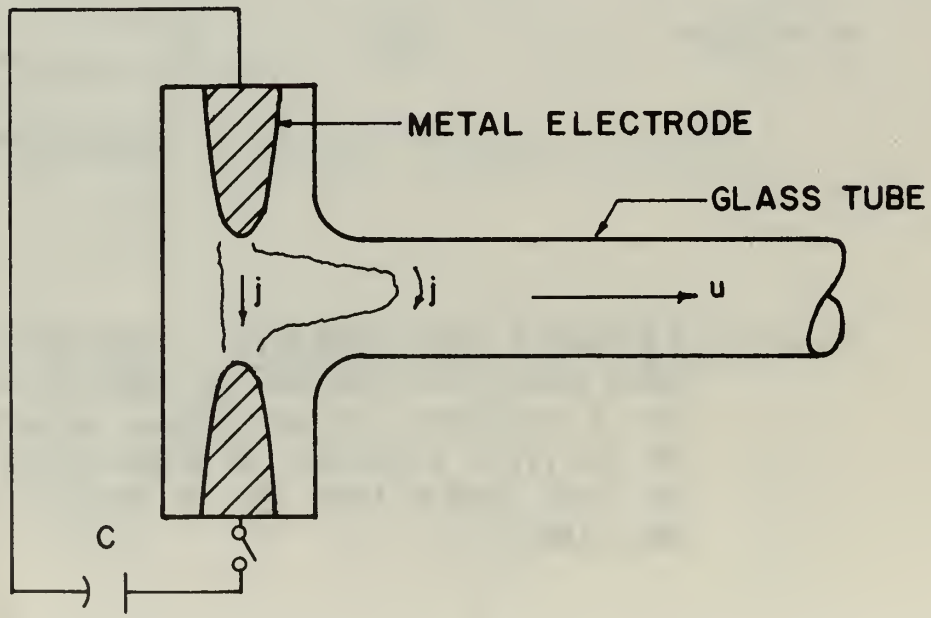

Figure 2b. T-Tube Plasma Accelerator

Figure 2. TWO ACCELERATORS

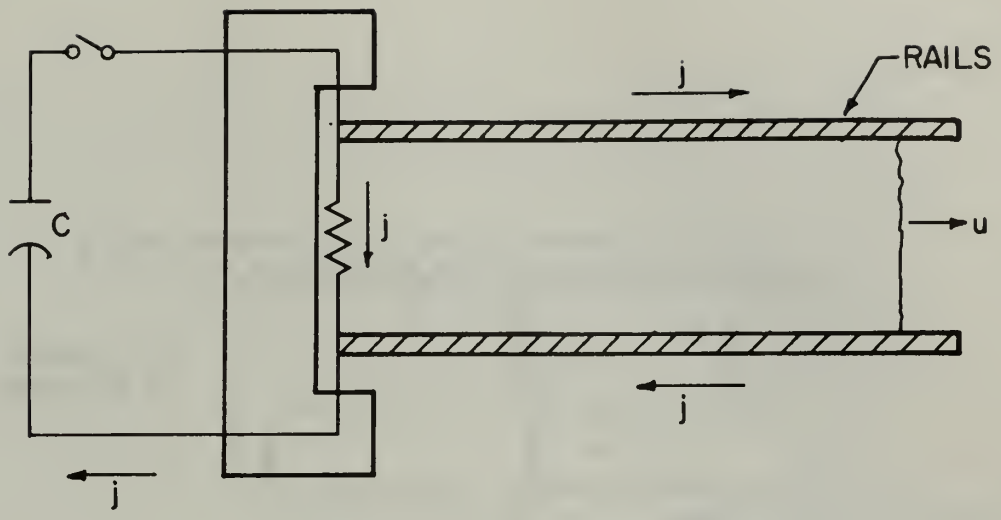

Figure 3a. Rail Accelerator

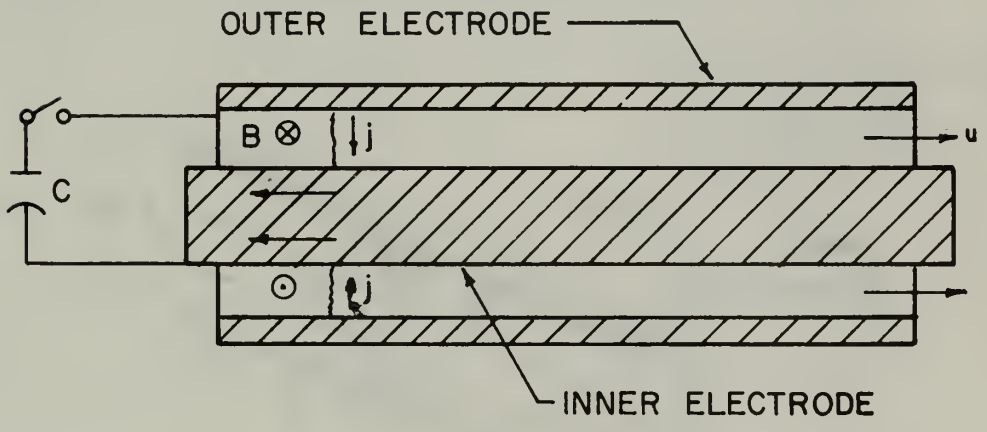

Figure 3b. Coaxial Accelerator

Figure 3. RAIL AND COAXIAL ACCELERATORS

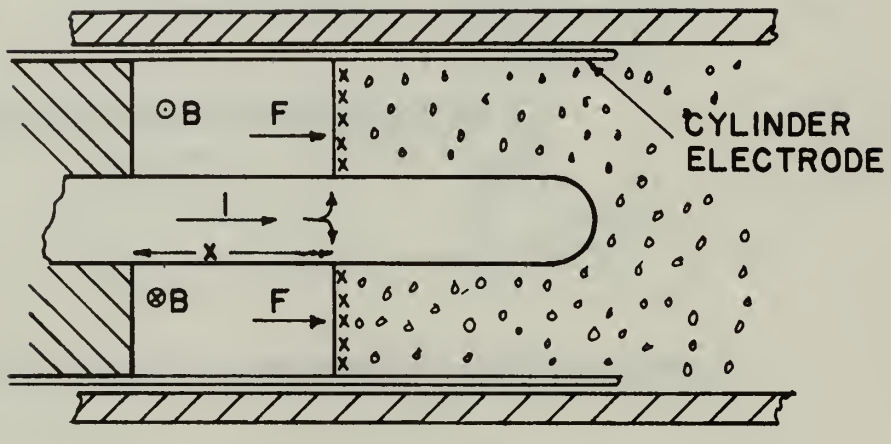

Figure 4a. Snowplow Model

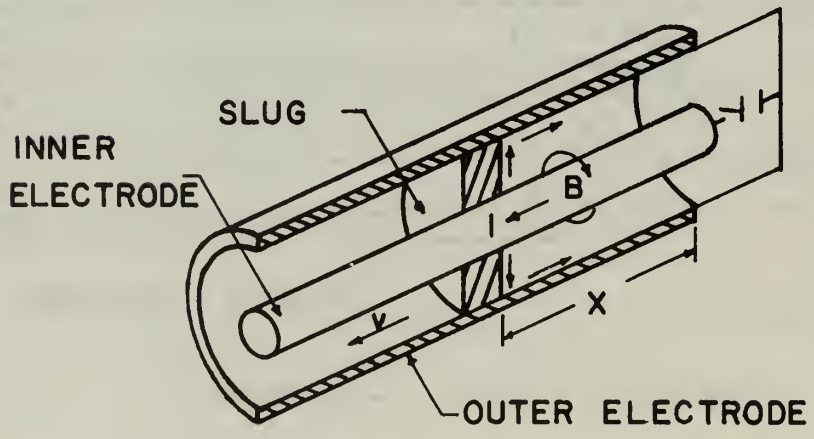

Figure 4b. Slug Model

Figure 4. PLASMA MODELS

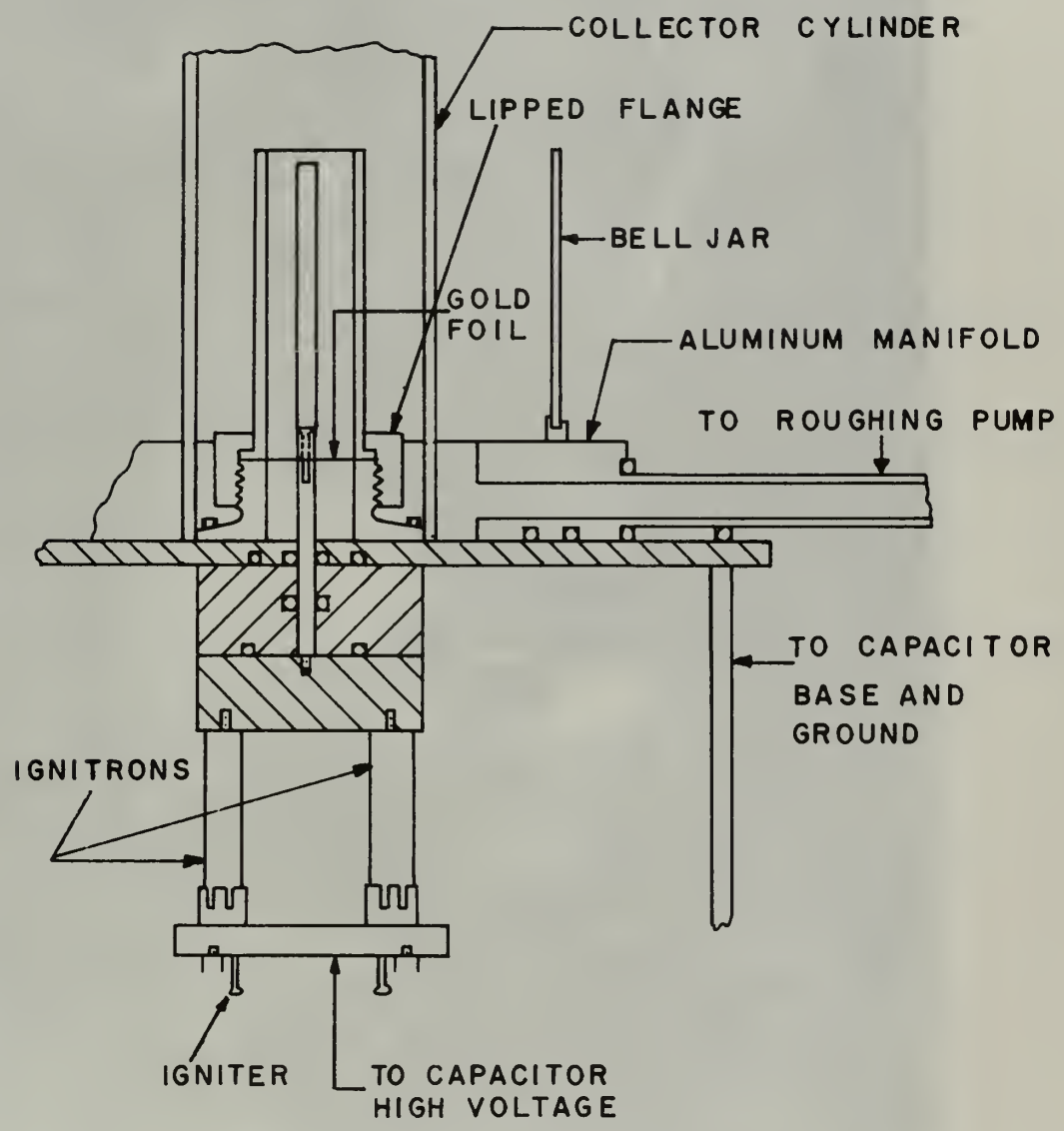

Figure 5. PLASMA ACCELERATOR

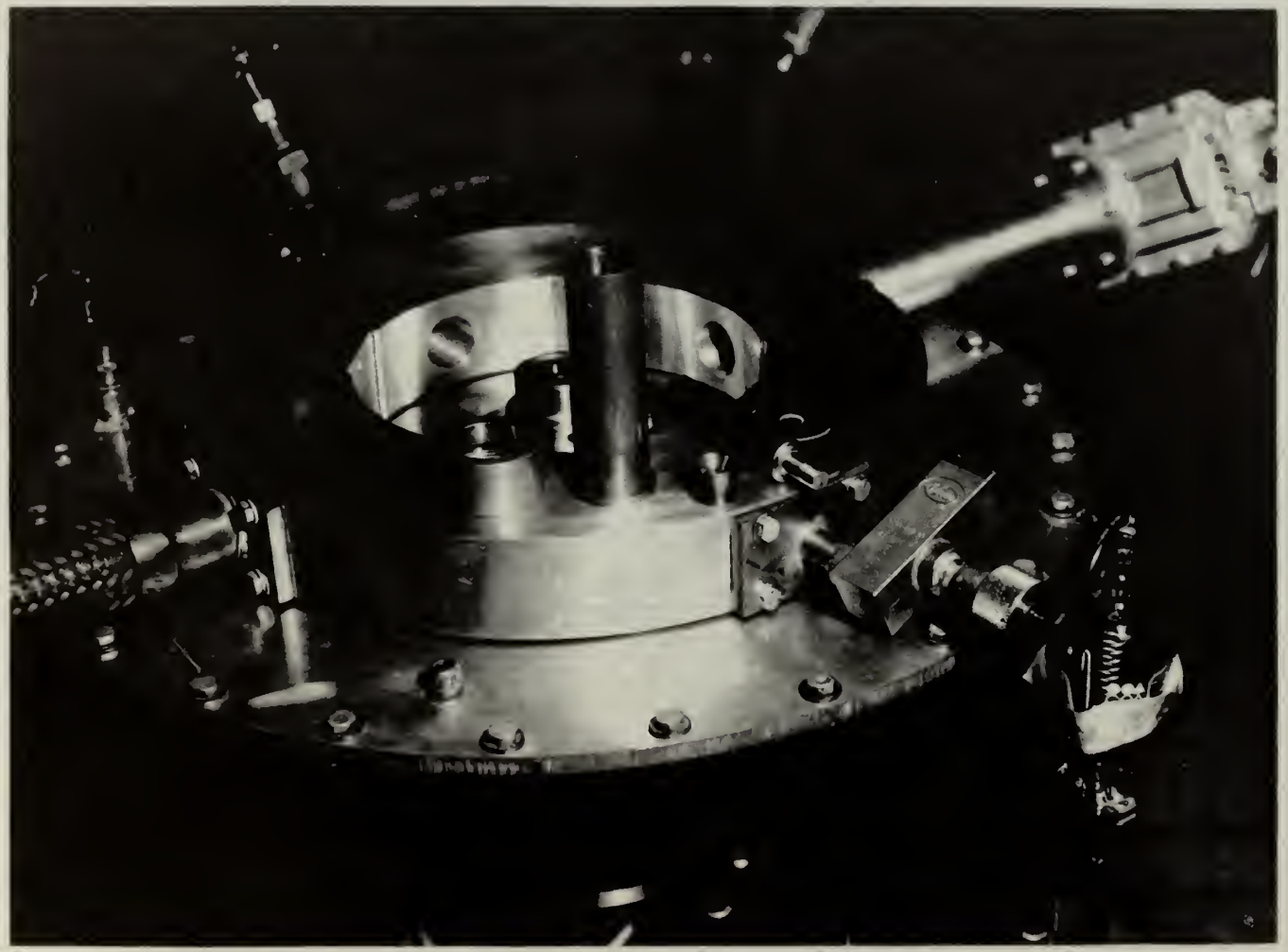

Figure 6. DISASSEMBLED ELECTRODES

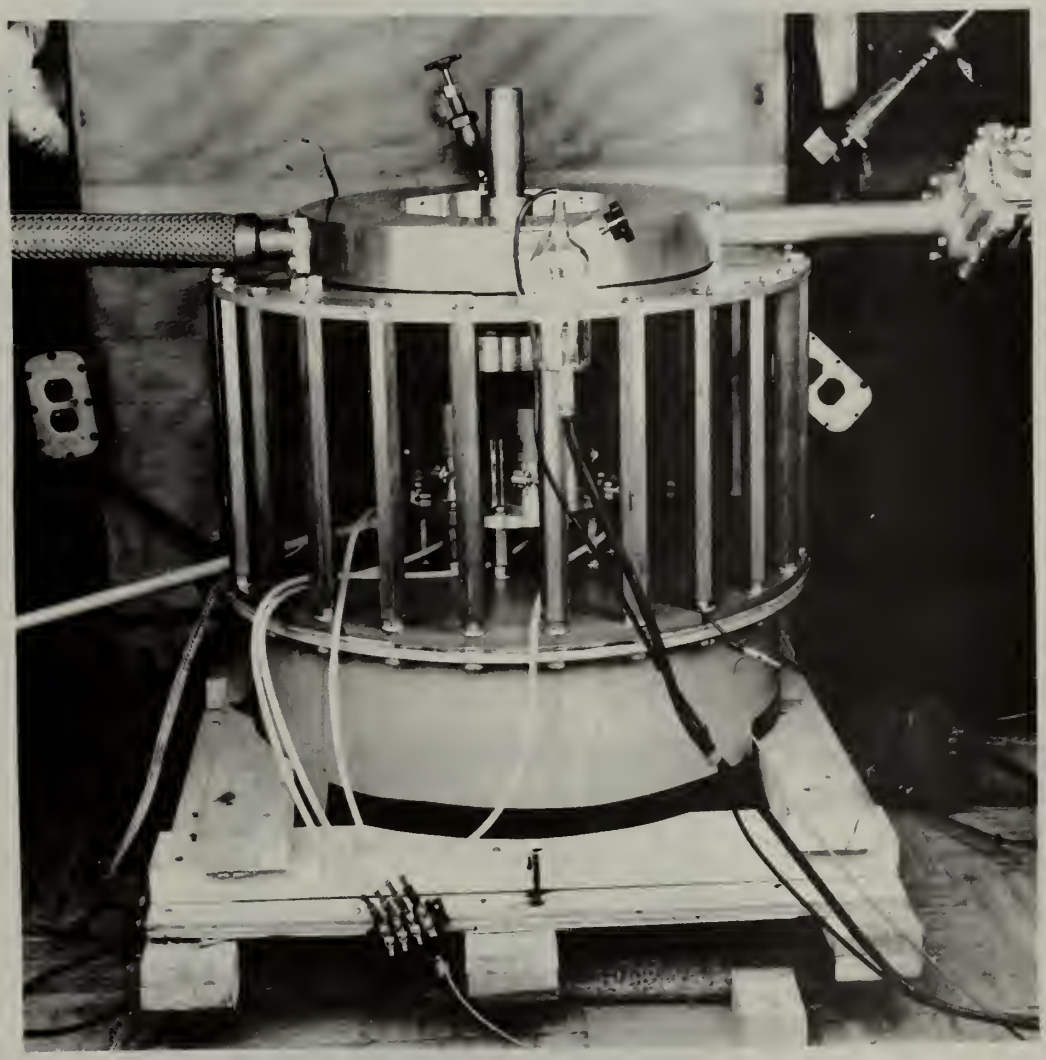

Figure 7.

ELECTRODES

IGNITRONS

CAPACITOR

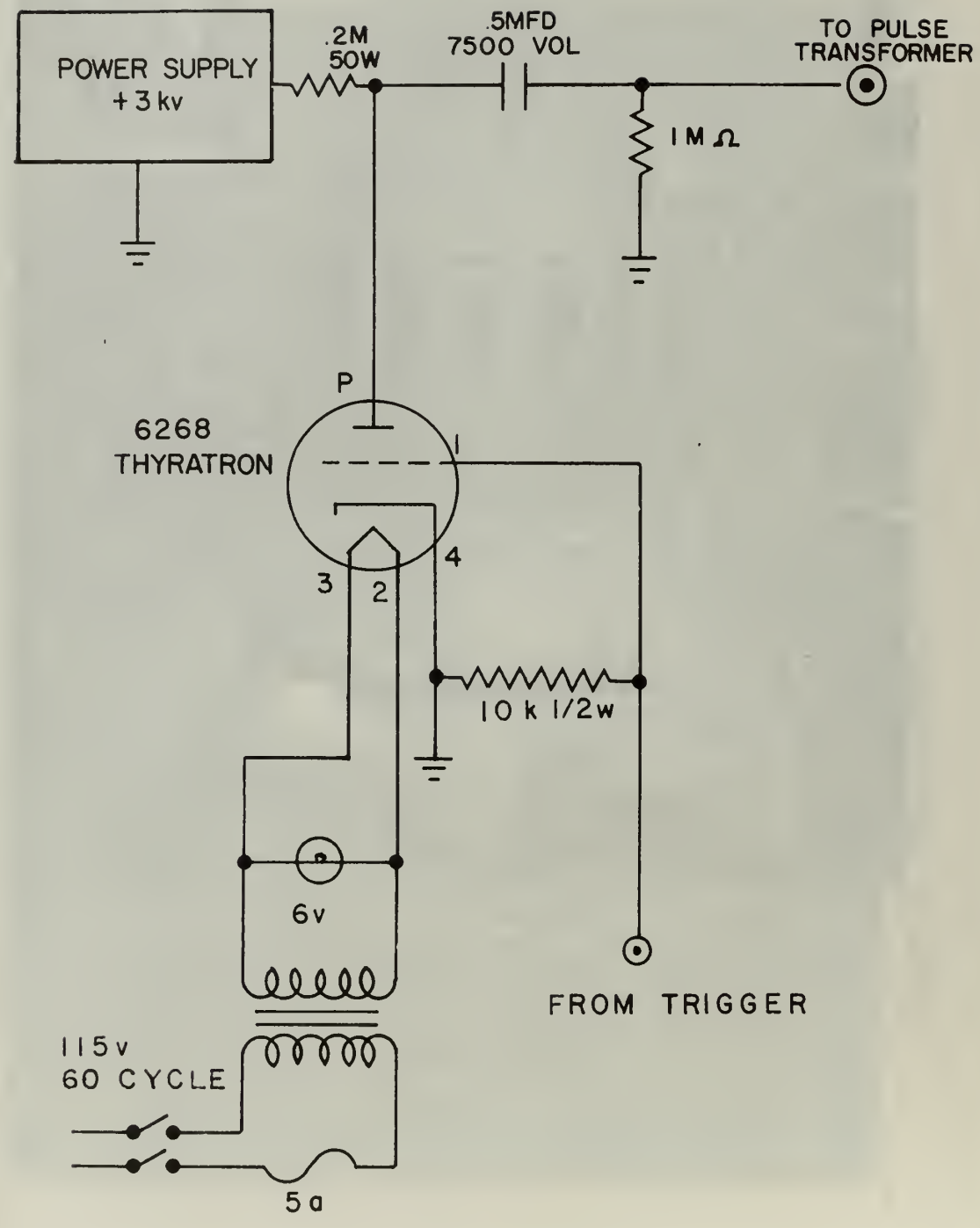

Figure 8. IGNITRON PULSER

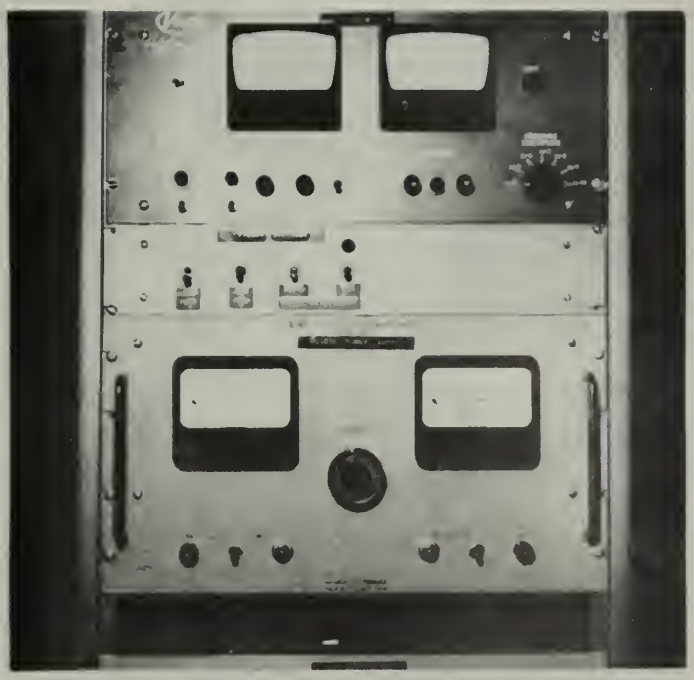

Figure 9a. Vacuum Controls and Pulser Power Supply

Figure 9b. Pulser Control Panel and Pulse Transformer

Figure 9. CONTROL PANELS AND PULSE TRANSFORMER

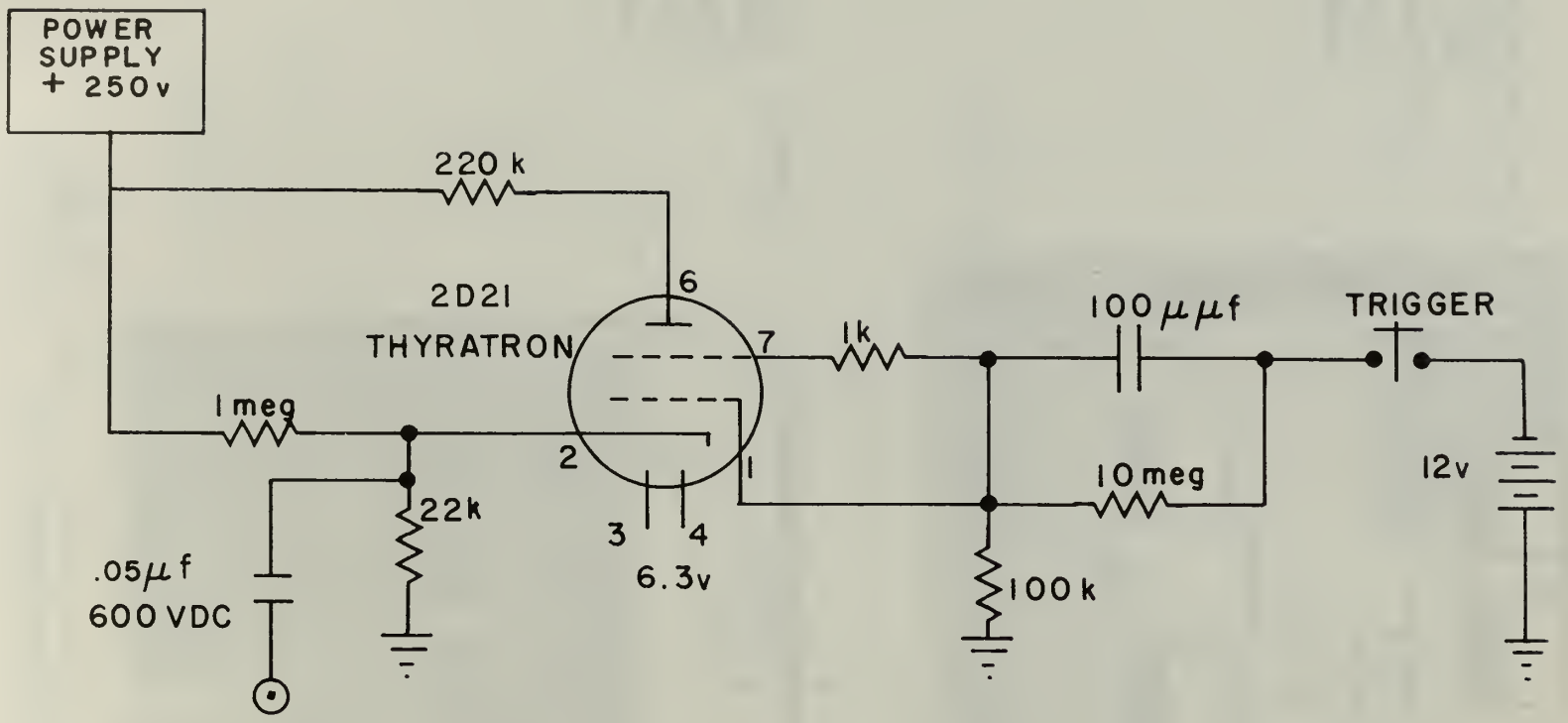

Figure 10. CAPACITOR DISCHARGE TRIGGER

Figure IIa. Pulser Trigger

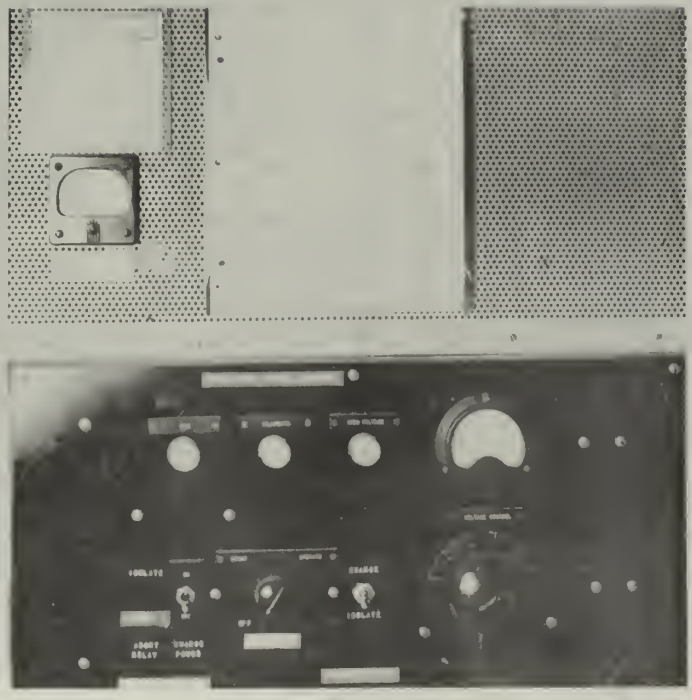

Figure IIb. High Voltage Power Supply

Figure II. CAPACITOR CHARGE AND DISCHARGE

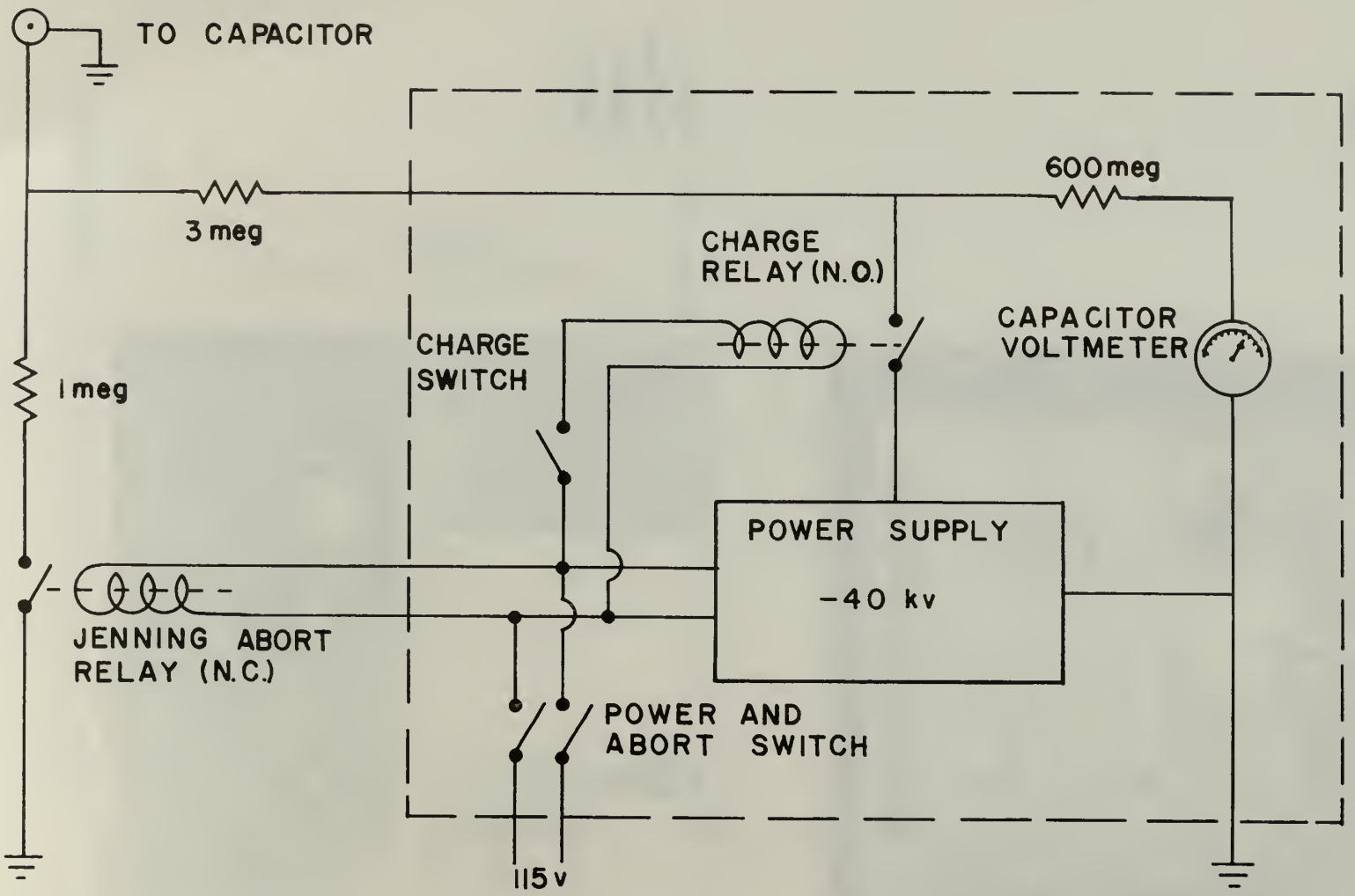

Figure 12. HIGH VOLTAGE SYSTEM

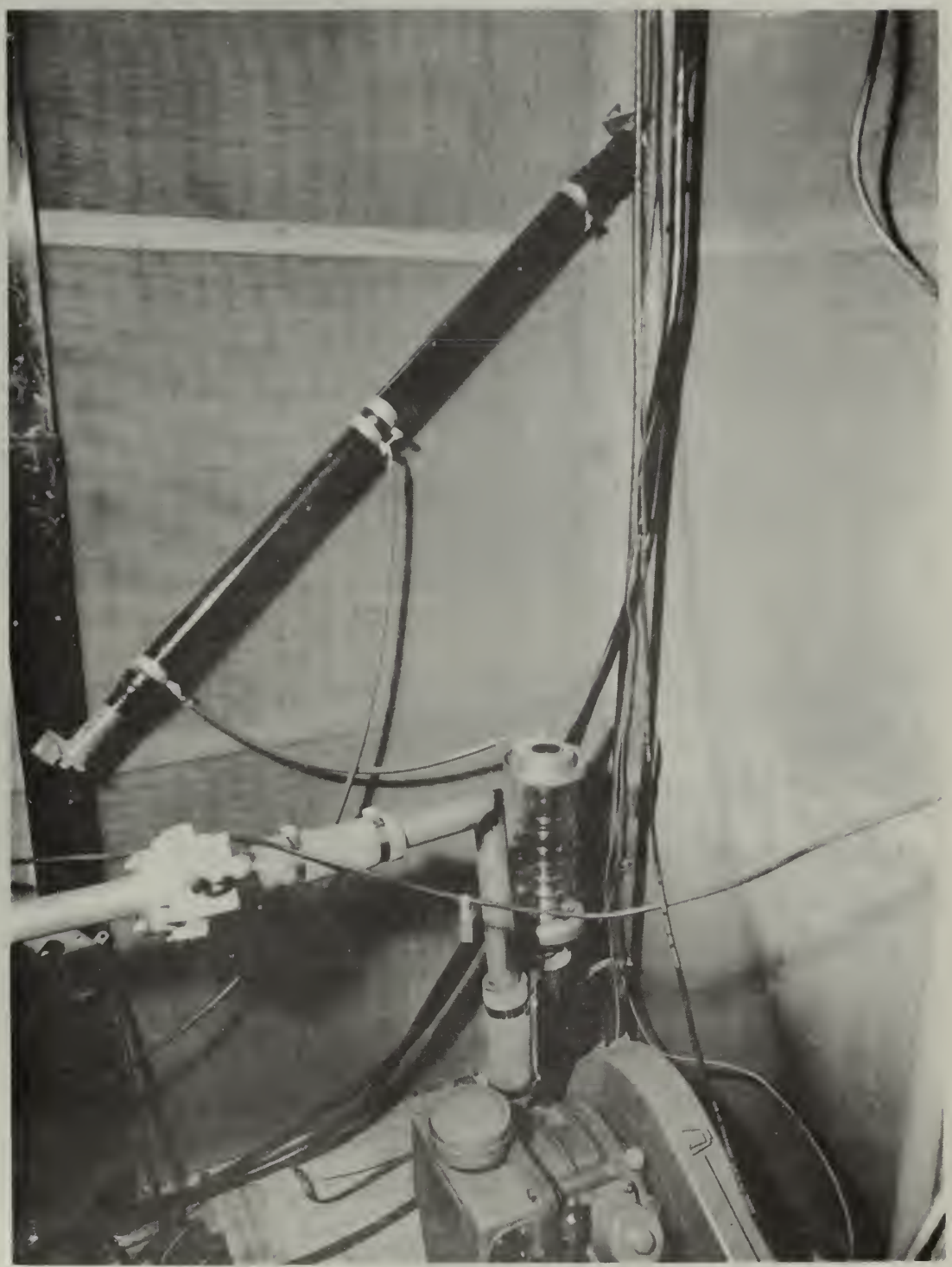

Figure 13. RESISTORS AND RELAY

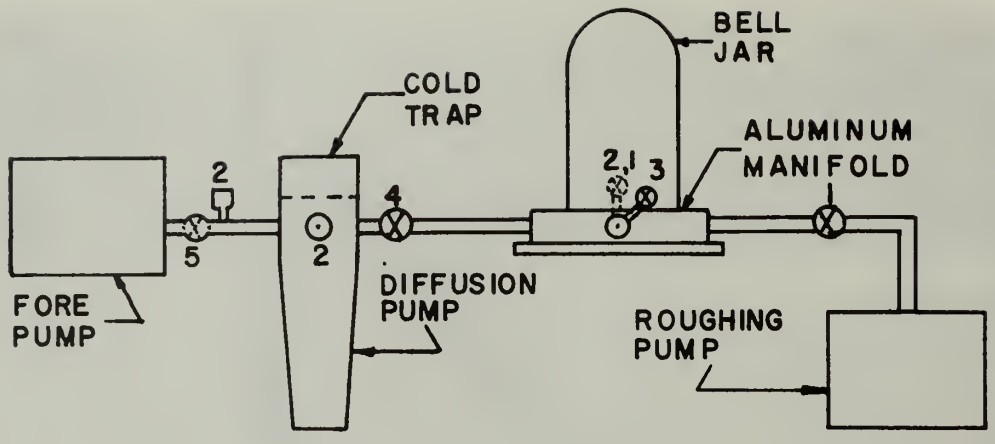

SIDE VIEW

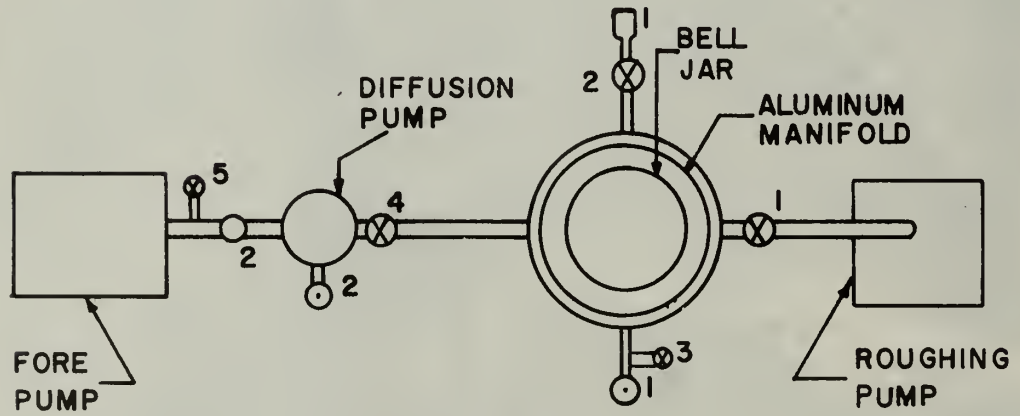

TOP VIEW

⊗ - VALVE

⊙ - IONIZATION GAUGE

⊓ - THERMOCOUPLE

Figure 14. VACUUM SYSTEM

Figure 15a. Fore Pump and Diffusion Pump

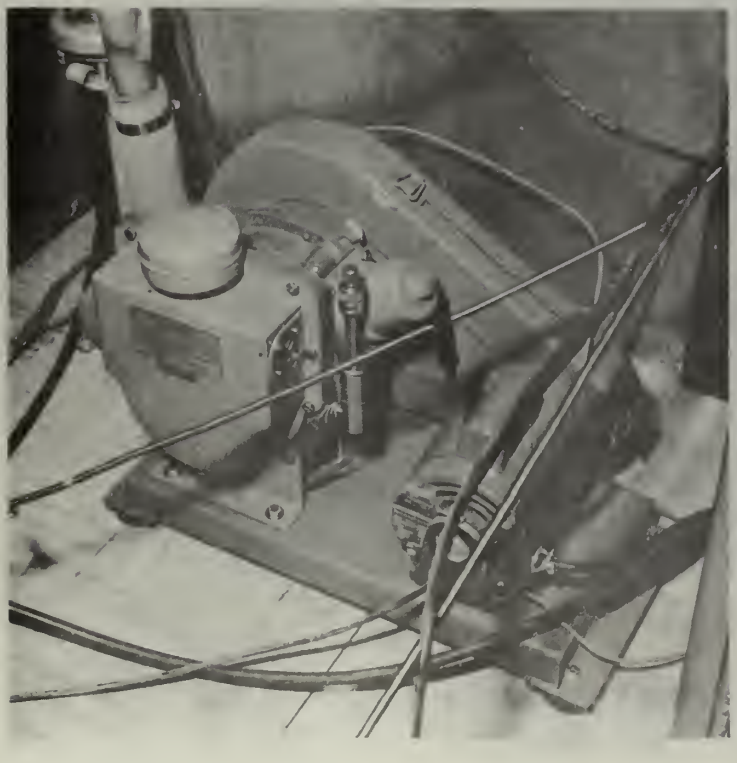

Figure 15b. Roughing Pump

Figure 15. VACUUM PUMPS

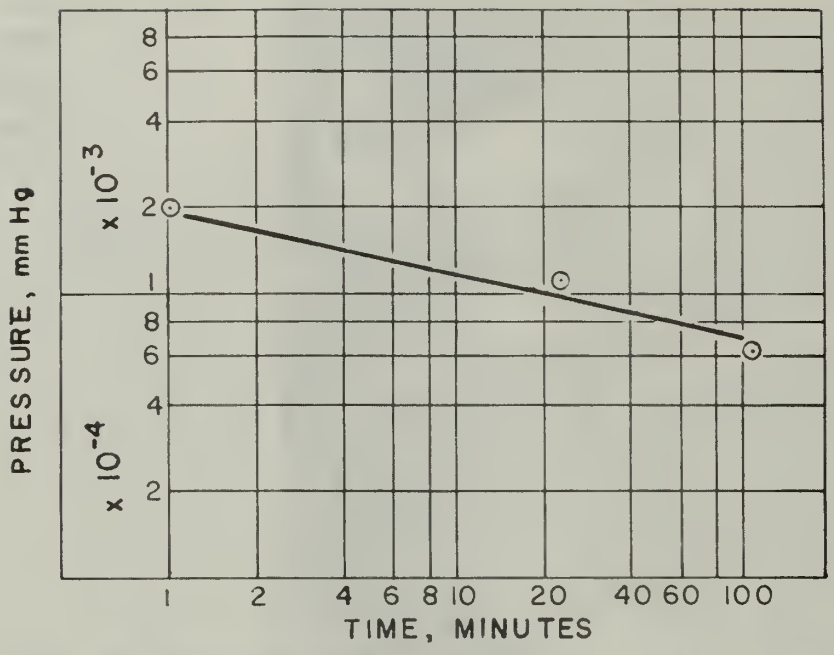

Figure 16 a. Pressure in Test Section vs Time

Figure 16b. Water Flow Switch

Figure 16. SYSTEM PRESSURE vs TIME AND WATER FLOW SWITCH

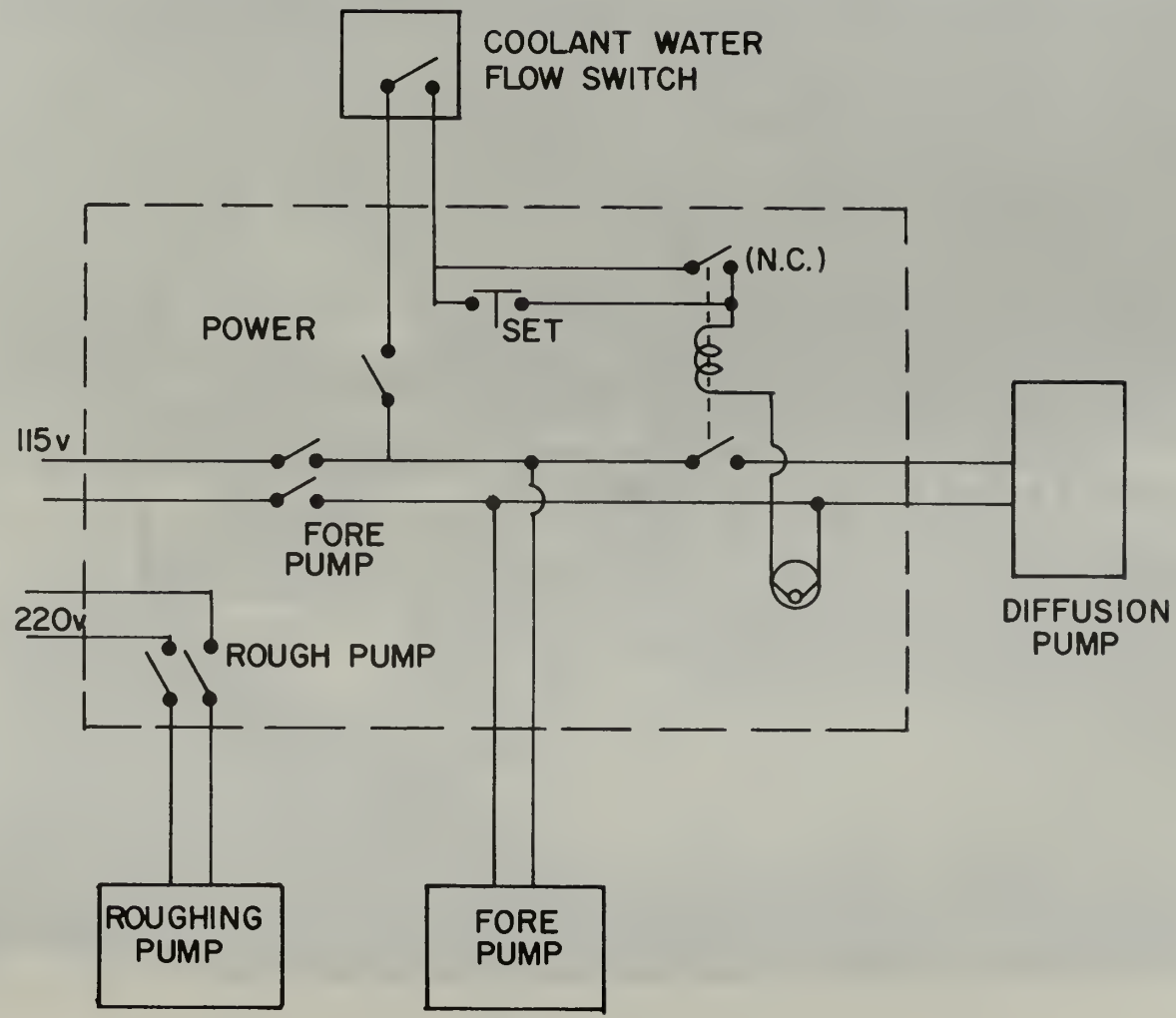

Figure 17. VACUUM CONTROLS

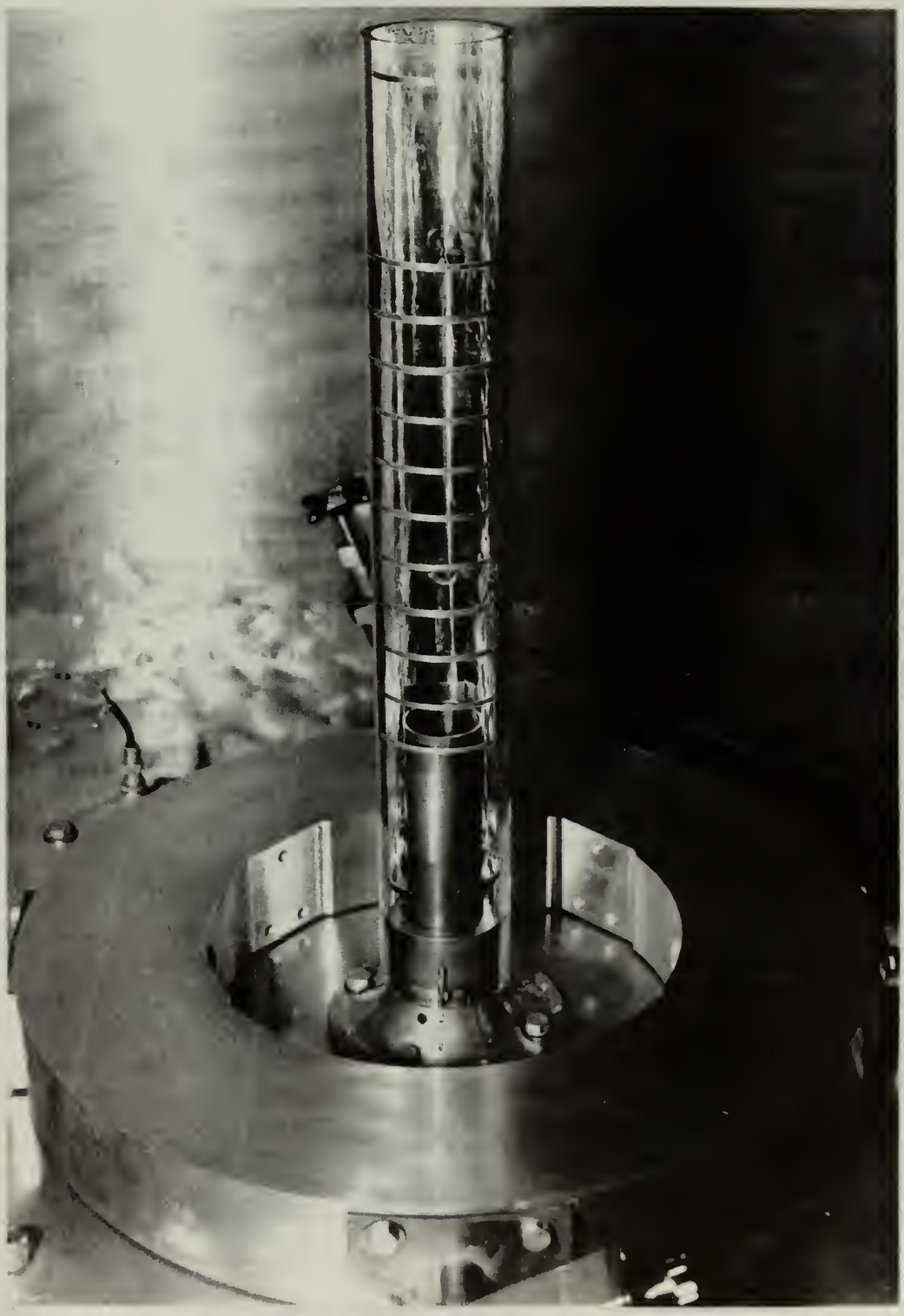

Figure 18. ASSEMBLED ELECTRODES AND COLLECTOR TUBE

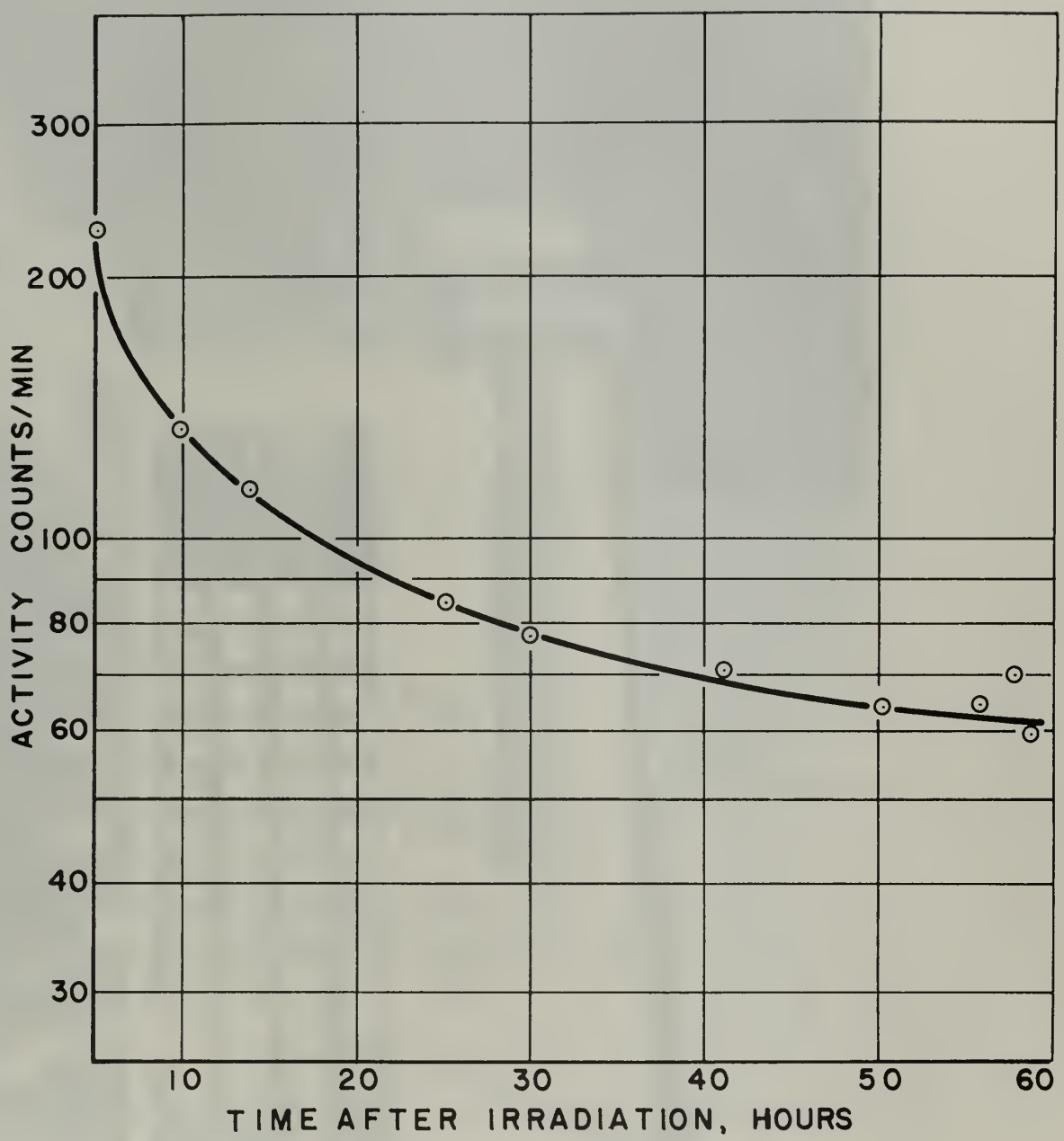

Figure 19. BACKGROUND DECAY

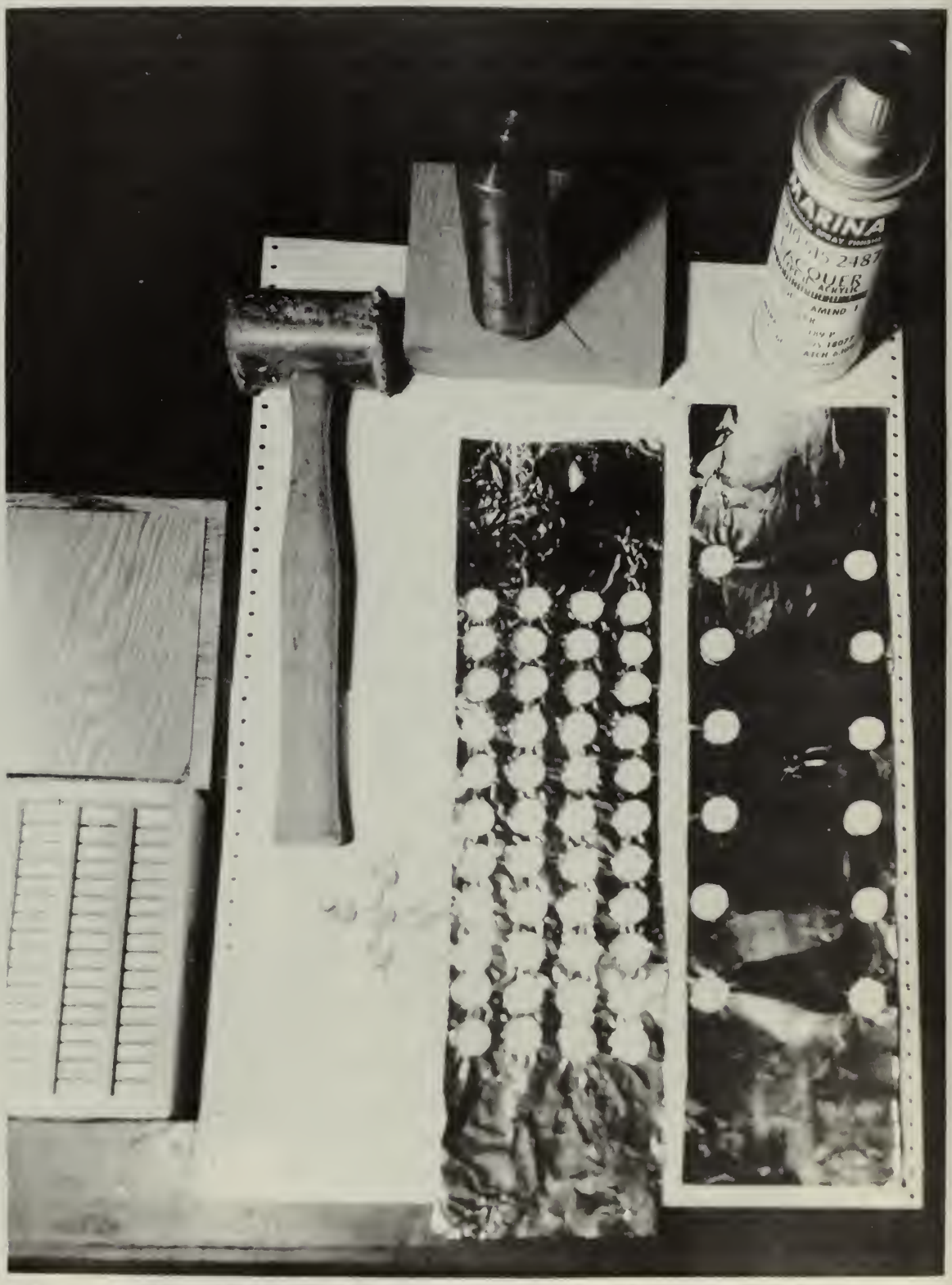

Figure 20. SAMPLE COLLECTION AND PREPARATION EQUIPMENT

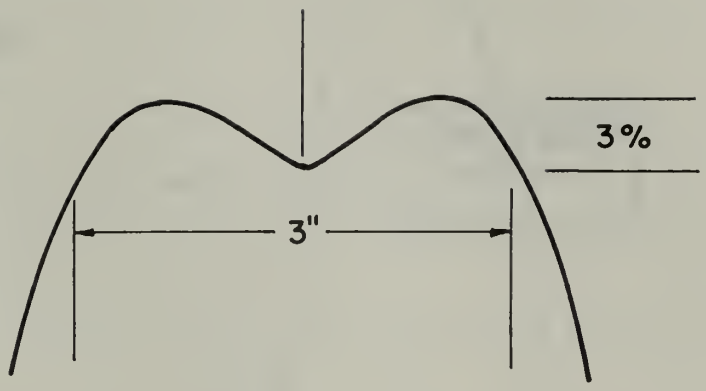

Figure 21a. Neutron Flux Distribution At Core Center of Reactor

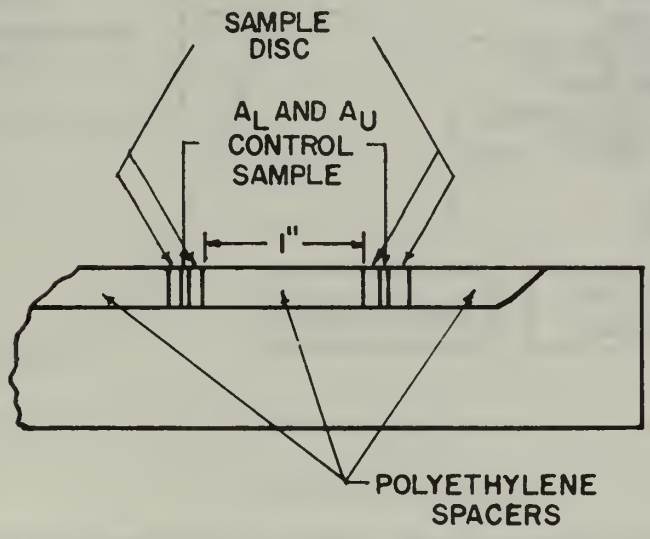

Figure 21b. Sample Disc And Control Sample Placement

Figure 21. SAMPLE PLACEMENT FOR IRRADIATION AND FLUX DISTRIBUTION AT CORE CENTER

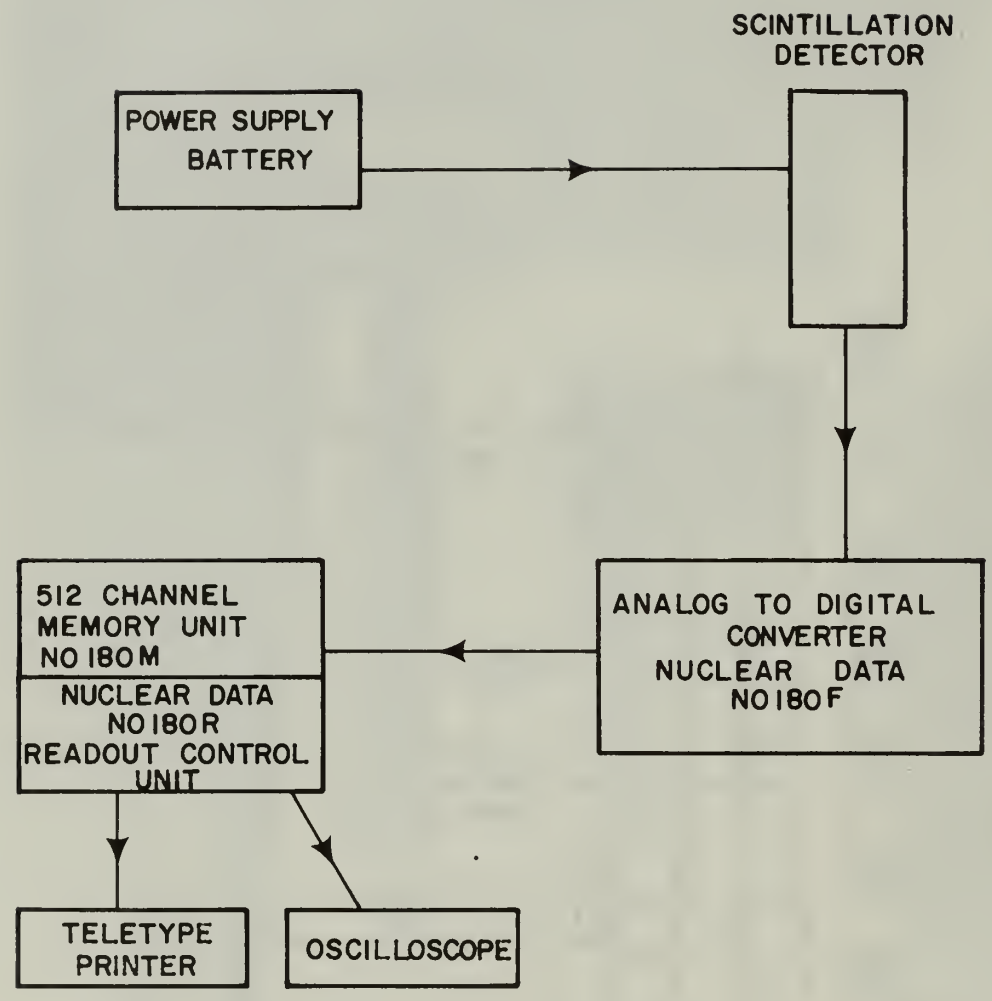

Figure 22. DETECTION AND COUNTING SYSTEM

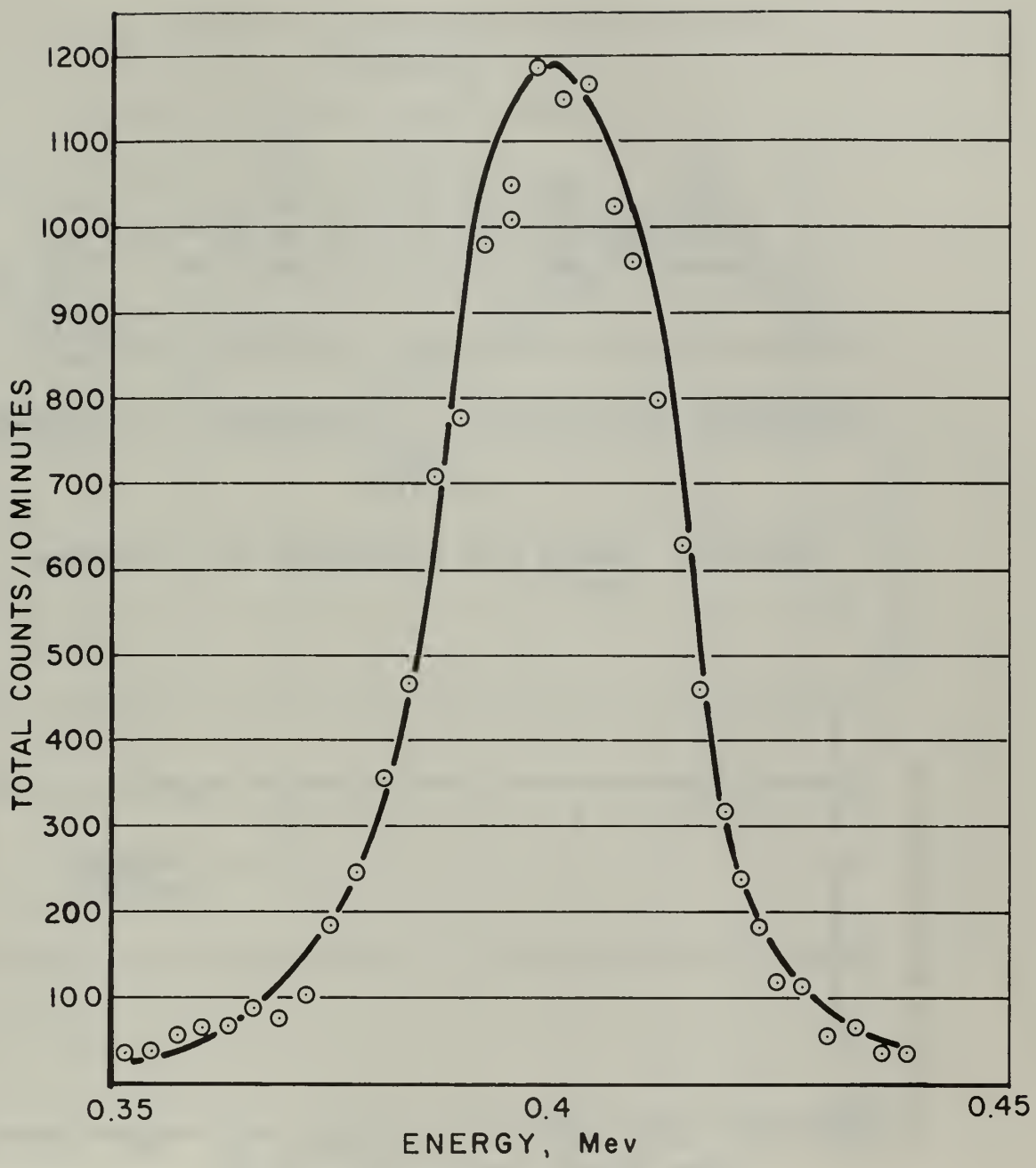

Figure 23. GOLD PEAK AS SEEN ON DETECTION EQUIPMENT

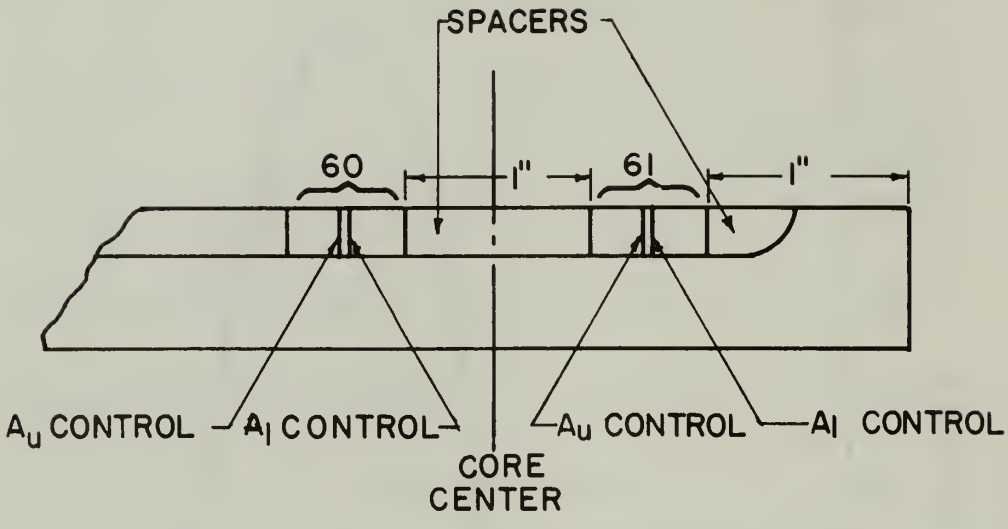

Figure 24a. Sample Disk Arrangement for Irradiation, Shot 6

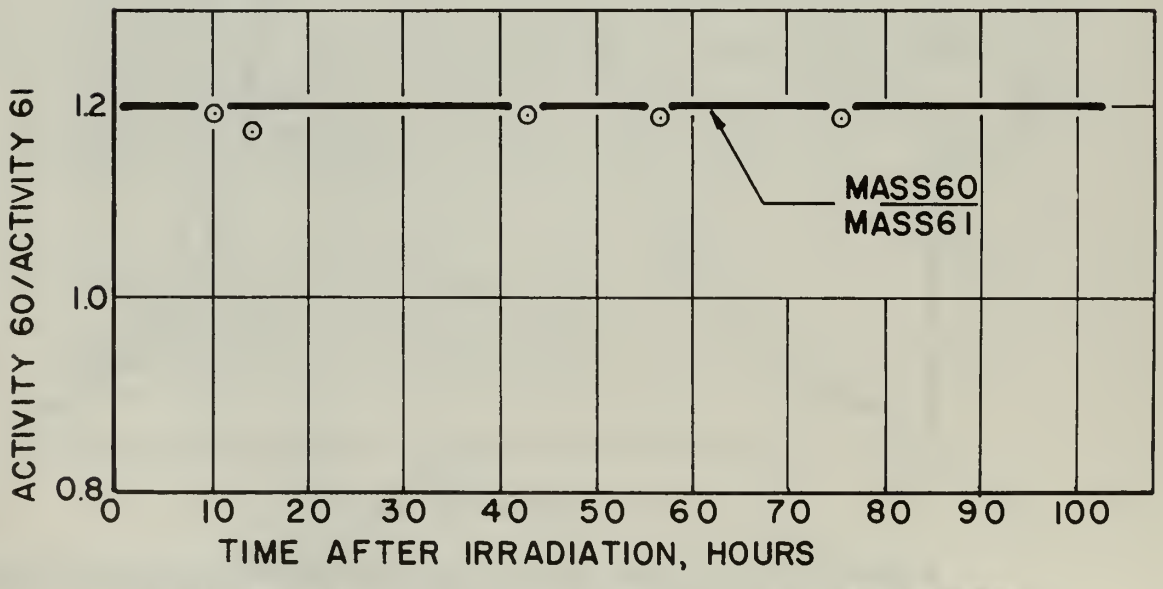

Figure 24b. A Comparison of the Ratios of the Masses of Control Samples 61 and 60 with the Ratios of their Activities

Figure 24. SAMPLE DISK ARRANGEMENT FOR IRRADIATION FOR SHOT 6 AND IRRADIATION FLUX RECEIVED BY CONTROL SAMPLES

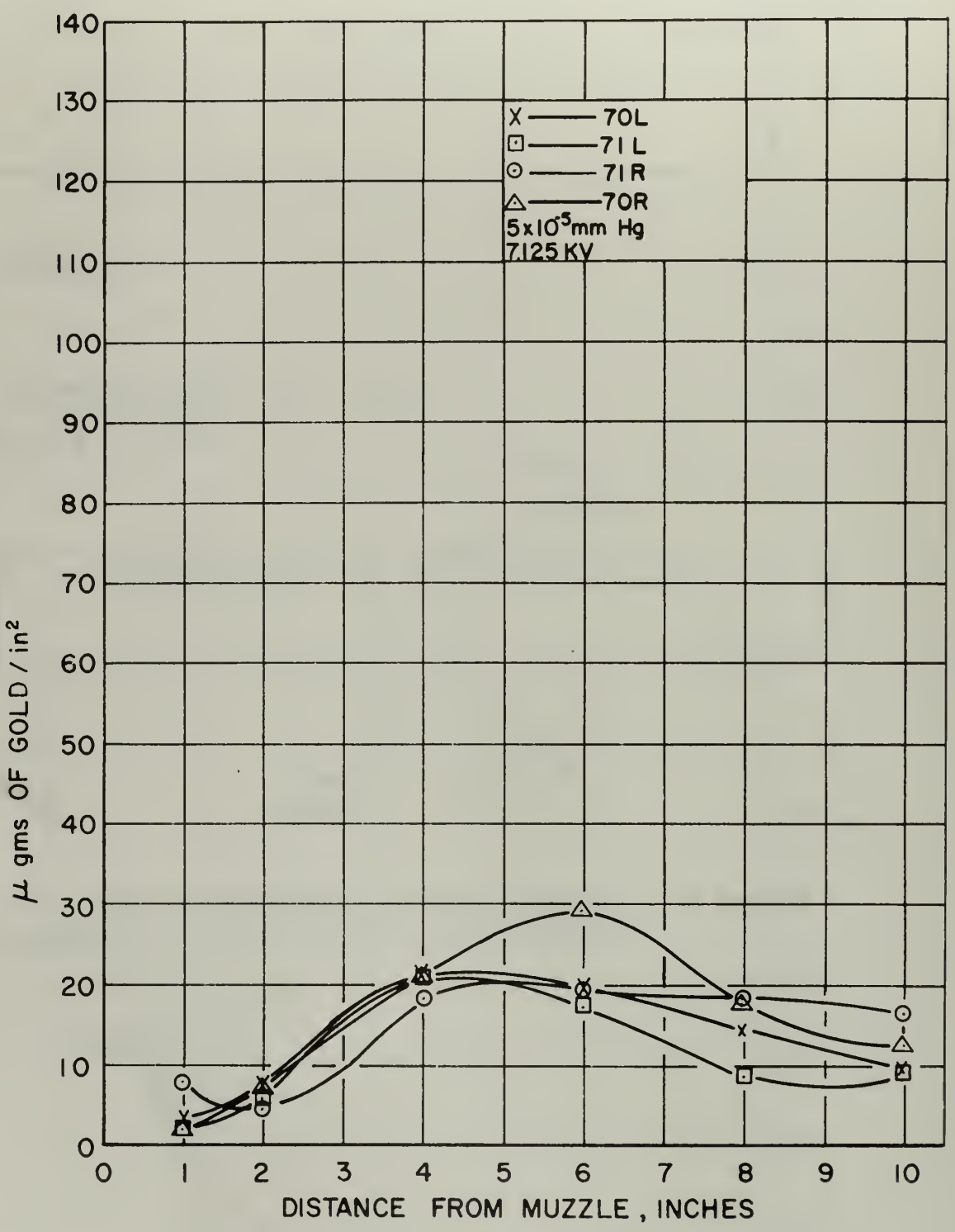

Figure 26. GOLD DISTRIBUTION SHOT 7

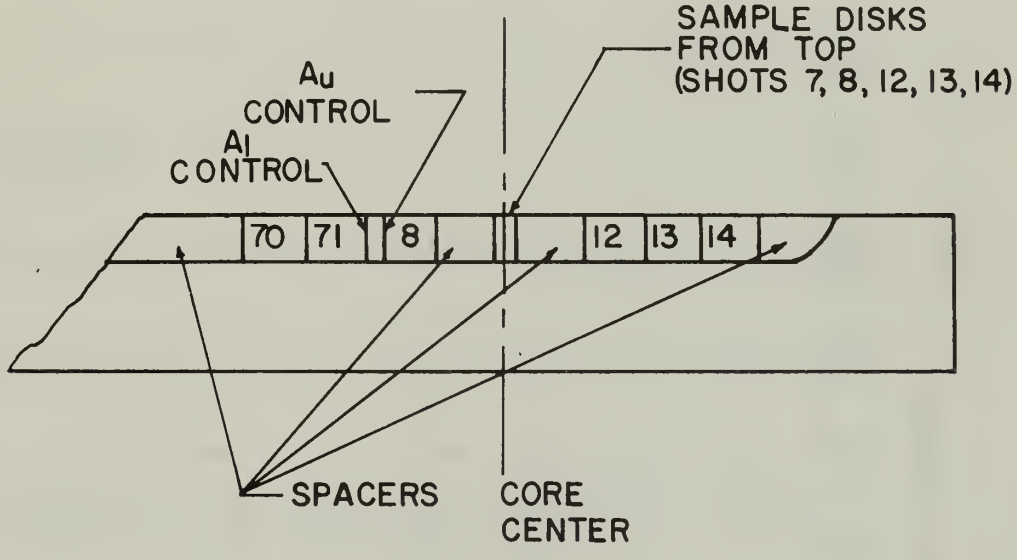

Figure 25. SAMPLE DISKS ARRANGED FOR IRRADIATION, SHOTS 7, 8, 12, 13, AND 14

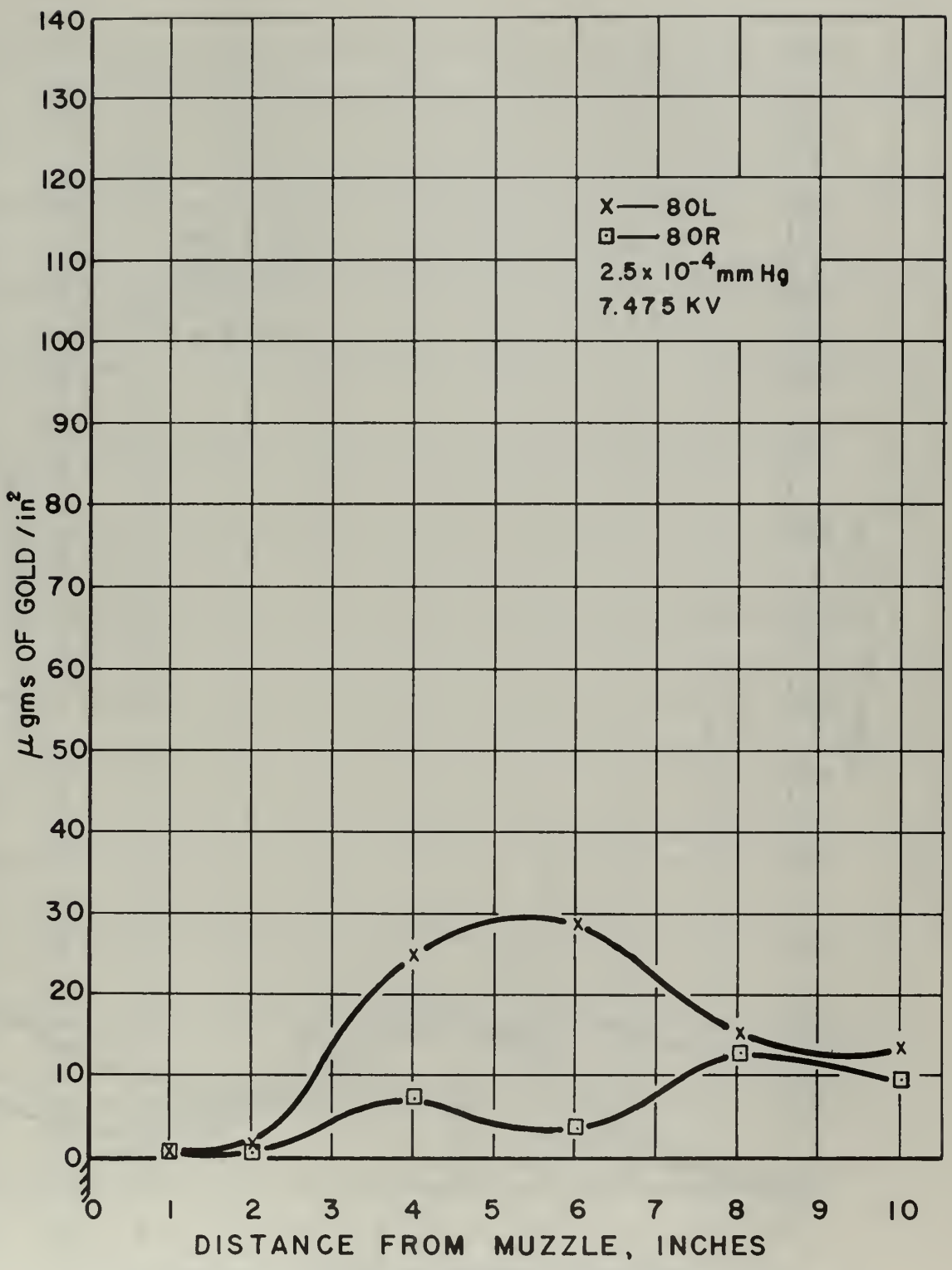

Figure 27. GOLD DISTRIBUTION SHOT 8

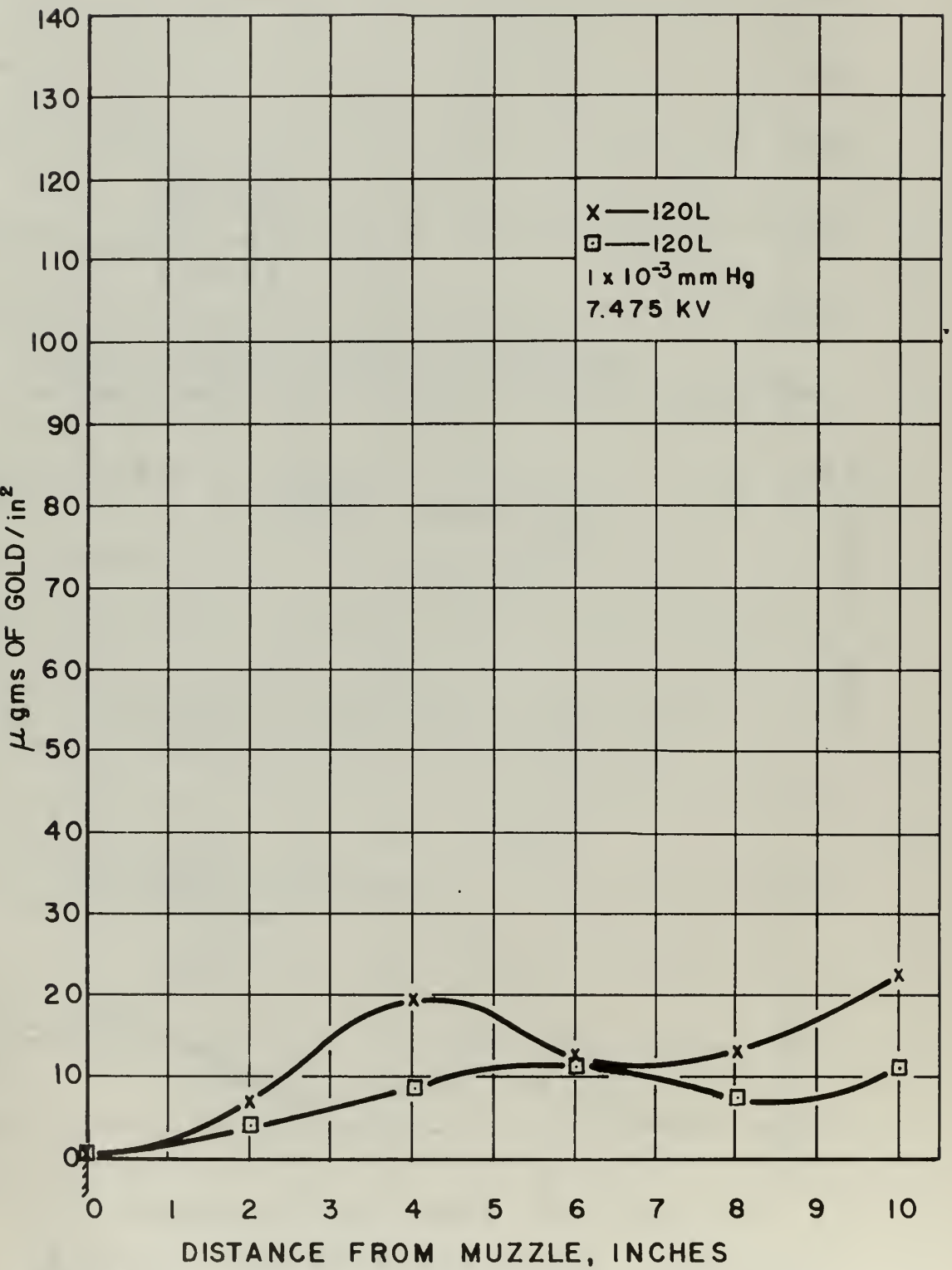

Figure 28. GOLD DISTRIBUTION SHOT 12

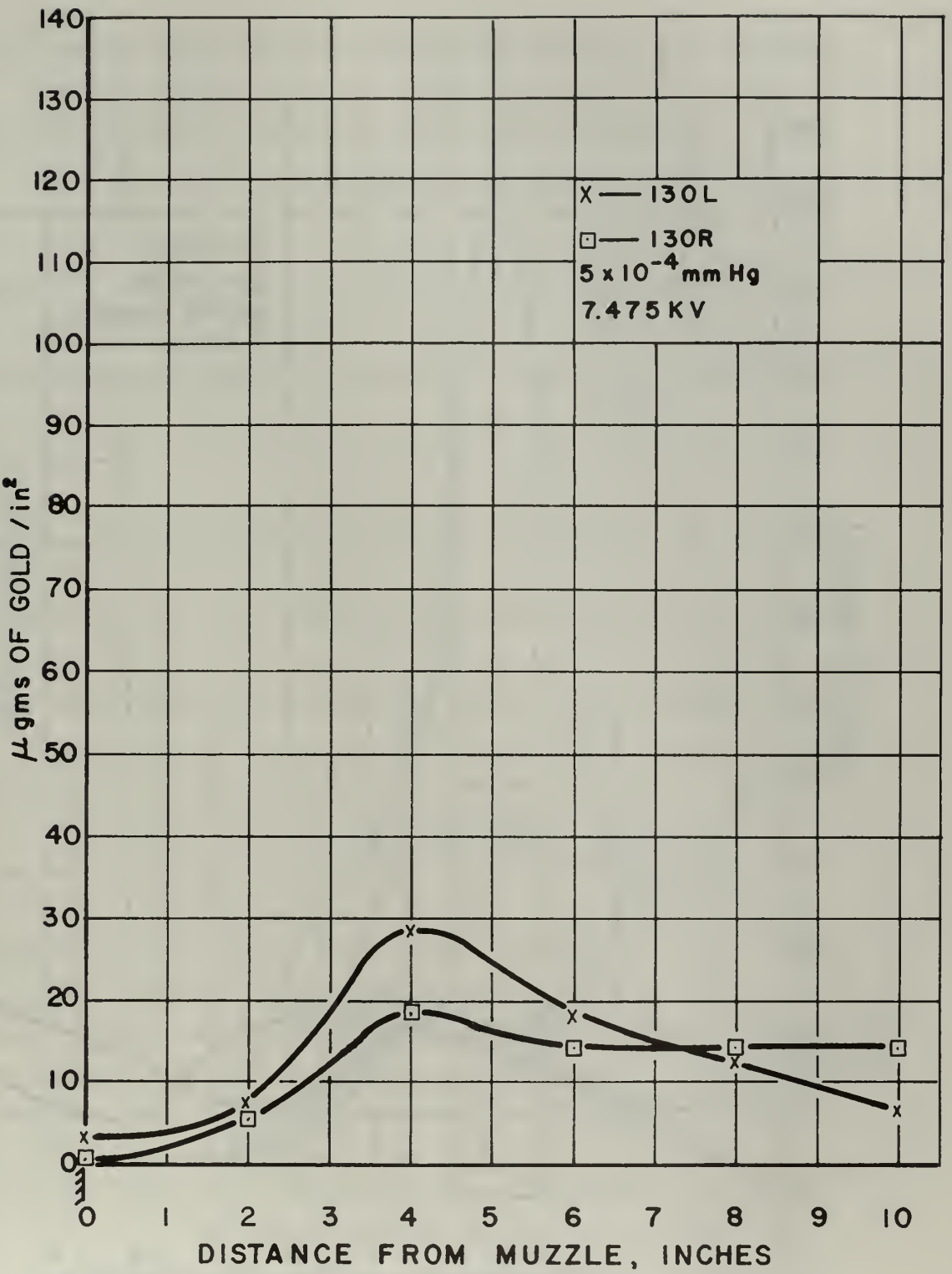

Figure 29. GOLD DISTRIBUTION SHOT 13

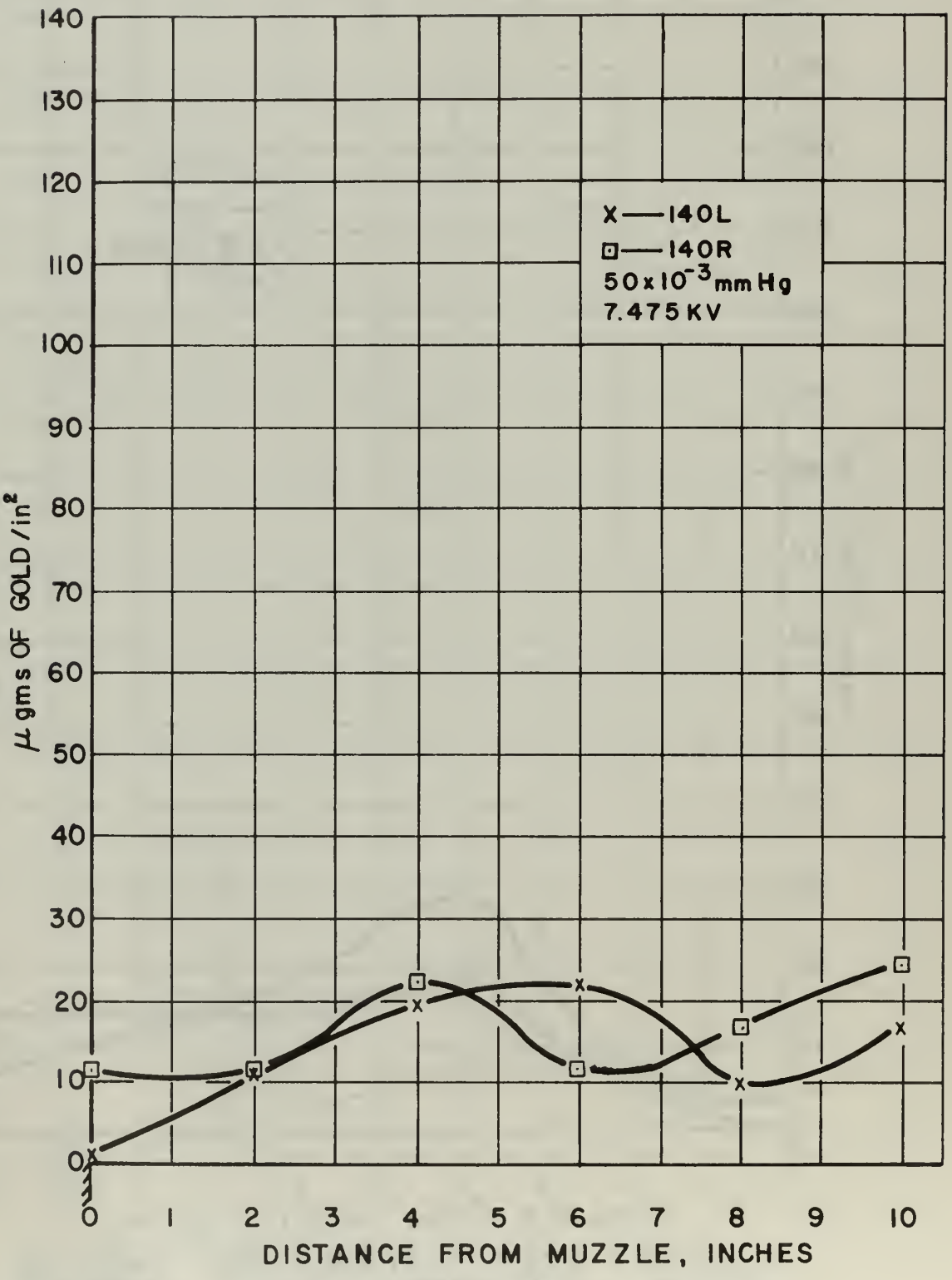

Figure 30. GOLD DISTRIBUTION SHOT 14

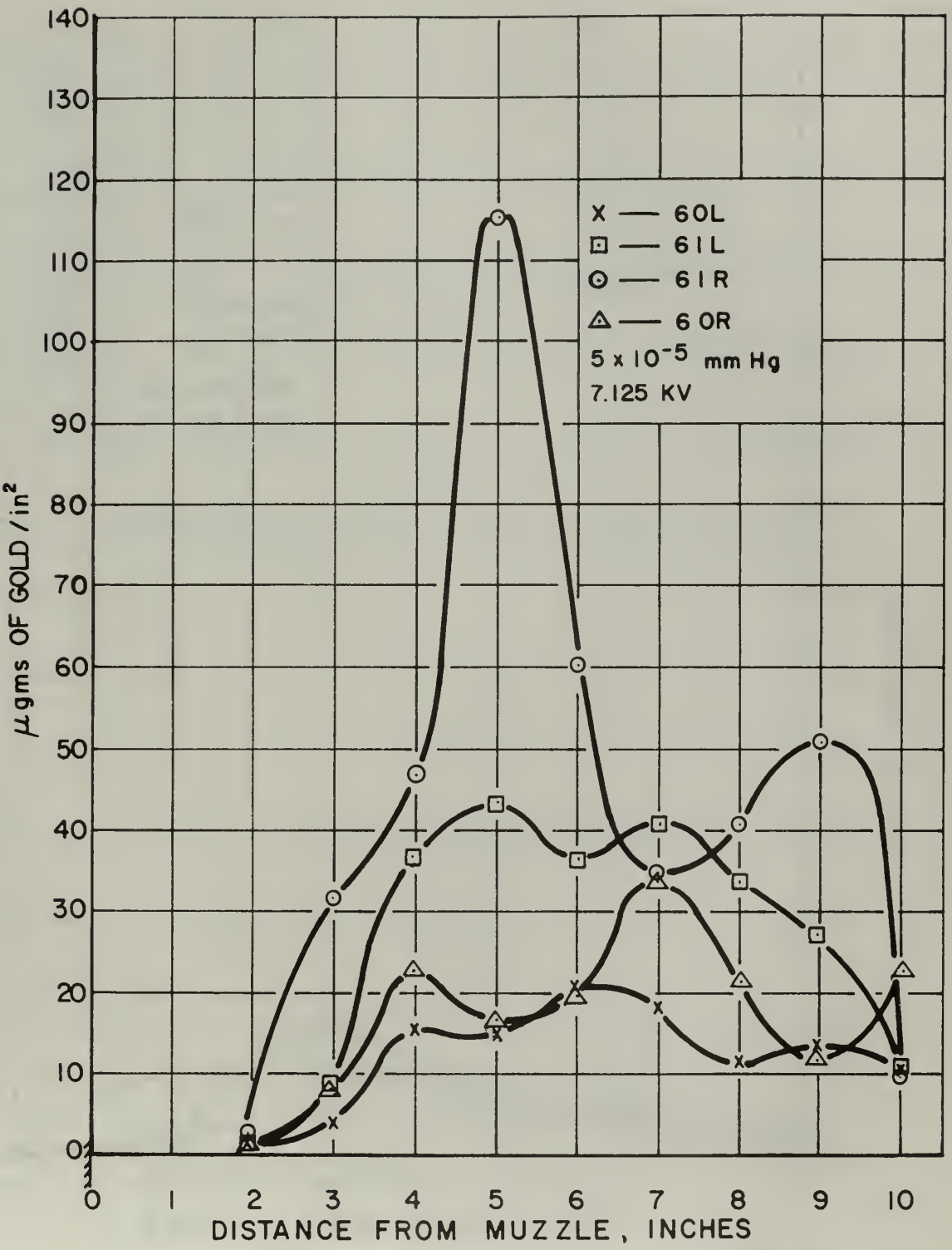

Figure 31. GOLD DISTRIBUTION SHOT 6

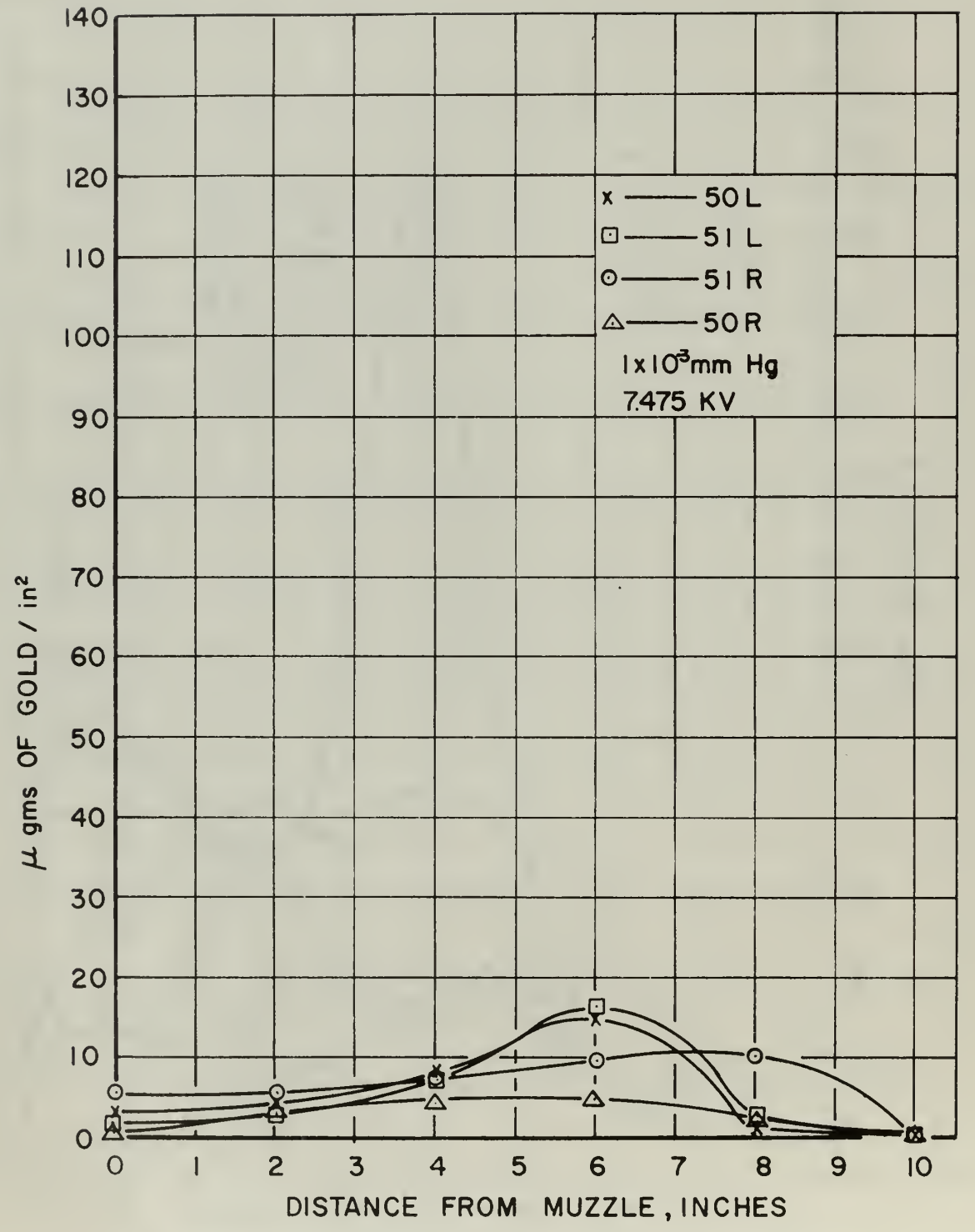

Figure 32. GOLD DISTRIBUTION SHOT 5

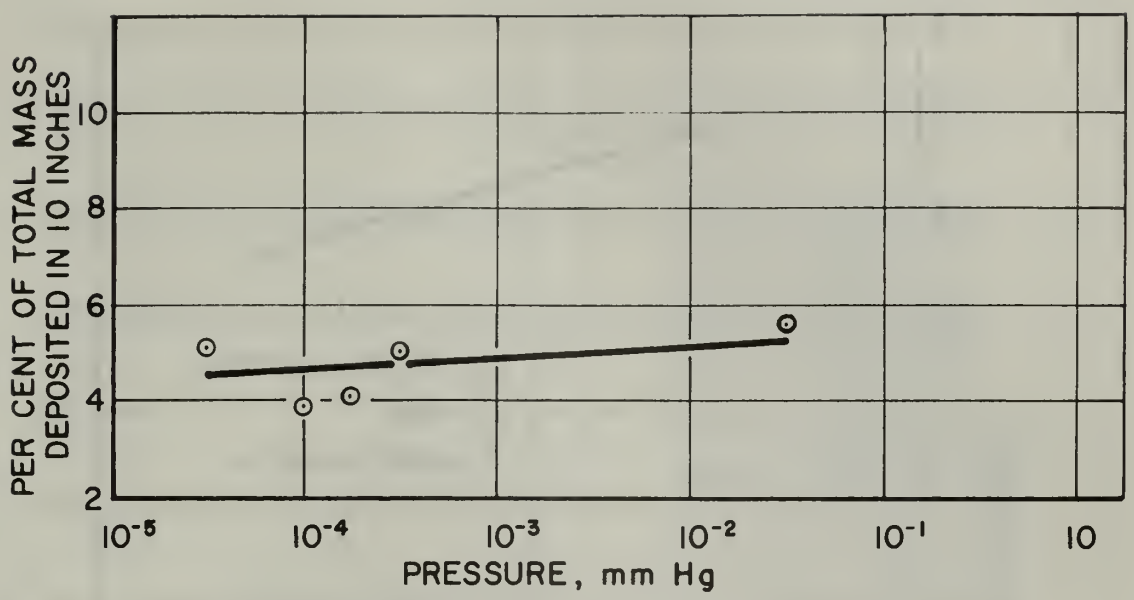

Figure 33a. Mass Deposited In 10 Inches Of The Collector Sheet Versus Exhaust Pressure

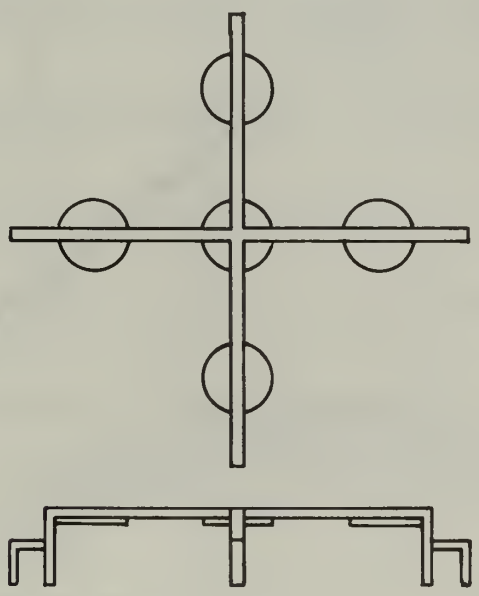

Figure 33b. Top Collector Configuration

Figure 33. MASS DEPOSITED VERSUS PRESSURE AND TOP COLLECTOR CONFIGURATION

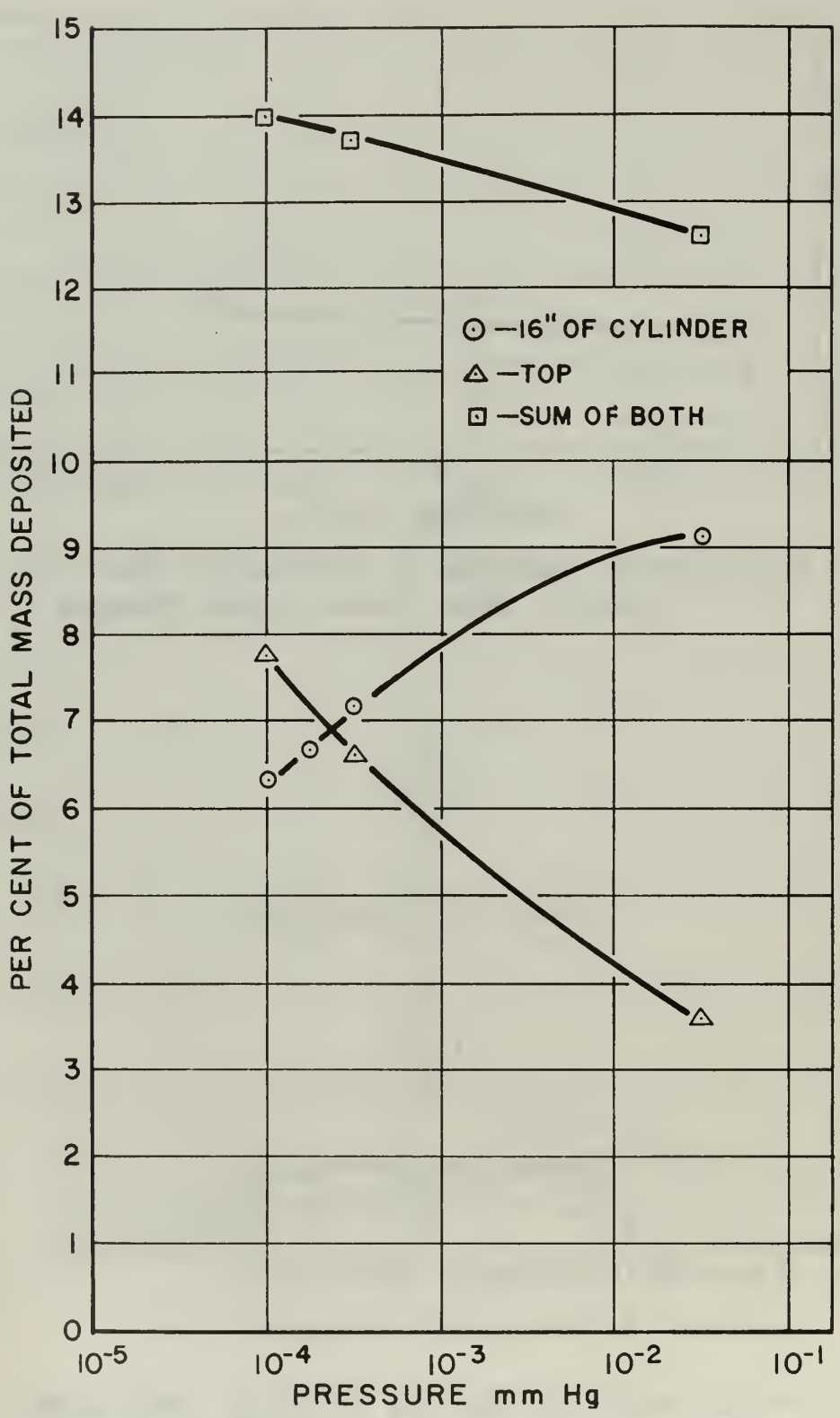

Figure 34. PERCENTAGE OF TOTAL MASS COLLECTED ON CYLINDER WALLS, AND TOP, AND THE SUM OF BOTH

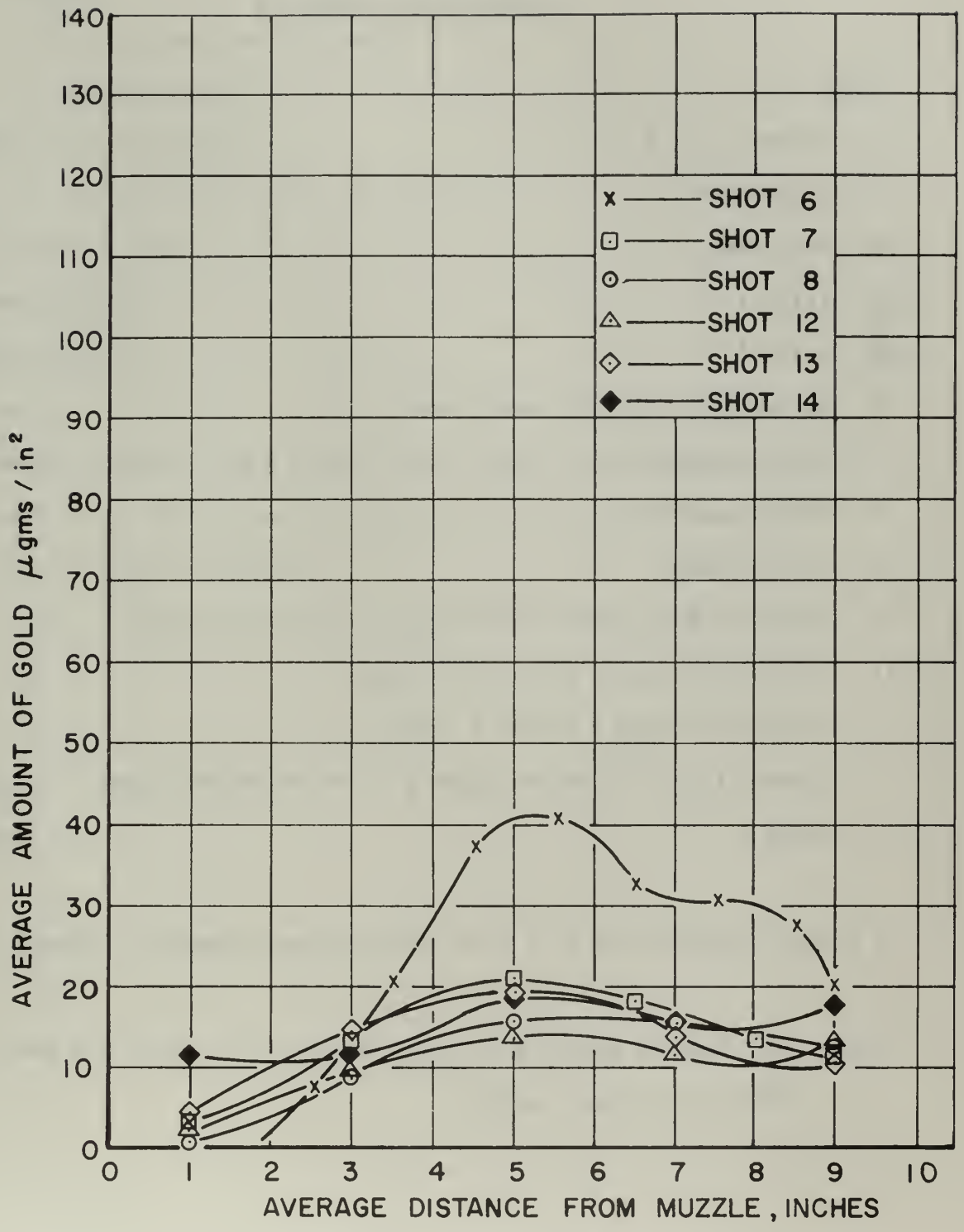

Figure 35. AVERAGE GOLD DISTRIBUTION

APPENDIX A

VACUUM SYSTEM OPERATION

START

1 - Valves 1, 2, 3, 4, 5	Closed
2 - Roughing Pump	On
3 - Fore Pump	On
4 - Valve 3	Open
5 - Valve 1	Open
6 - Vacuum gauge control panel power	On
7 - Thermocouple 1	On*
8 - Thermocouple 2	On
9 - Coolant Water	On, Full
10 - Diffusion Pump (when thermocouple 2 reads 40 microns)	On
11 - Ionization Gauge 2 (after 45 minutes)	On
12 - Ionization Gauge 1 (below 1 micron)	On
13 - Valve 4 (when ionization gauge 2 is in 10^{-6}mm Hg range)	Open
14 - Valve 1	Close

* Pressure should drop to 1 x 10^{-3}mm Hg in approximately 1 minute.

Note: The roughing pump and fore pump should be on while the gun is being cleaned and loaded.

SECURE

1 - Vacuum gauge control panel	Off
2 - Roughing Pump	Off
3 - Diffusion Pump	Off
4 - Coolant Water (after 15 minutes)	Off
5 - Fore Pump	Off
6 - Valve 5	Open
7 - Valve 2	Open

Note: Steps 5 and 6 should be performed simultaneously in order to insure that fore pump oil is not sucked into the diffusion pump.

APPENDIX B

FIRING PROCEDURE

1 - Vacuum System (through step 3, Appendix A)		Start
2 - All components under bell jar	Clean (with acetone)	
3 - Collector Tube		Load
4 - Electrodes		Load*
5 - Collector Tube	Place over outer electrode	
6 - All components under bell jar	Heat, approximately 5 min.	
7 - Bell Jar		Lower
8 - Vacuum System (from step 3, Appeindix A)		Operate

When desired vacuum is reached:

9 - Trigger Circuit		On
10 - Thyratron Heater		On
11 - Pulser Power		On
12 - Vacuum control panel power		Off
13 - Thermocouple leads	Disconnect from back of control panel	
14 - High Voltage (Pulser Circuit)		On, set 3 KV

FIRING

1 - Vacuum valve 3	Close
2 - Capacitor	Charge
3 - Vacuum valve 4	Close
4 - Trigger	Fire
5 - Capacitor Power Master	Off
6 - Capacitor Ground Rod	Install

*Inspect foil from muzzle end.

CAPACITOR POWER CONTROL

EMERGENCY

1 - Master	Off/Abort
2 - Capacitor ground rod	Install

CAPACITOR CHARGE

1 - Switches	Off, CCW
2 - Capacitor ground rod	Removed
3 - Master	On/Isolate
4 - Charge switch	Charge
5 - Filament control	Operate
6 - Voltage control	Set

Note: Do not exceed 0.55 microamps on the meter unless new ignitrons are installed.

When desired voltage is reached:

7 - Voltage control	Off
8 - Filament control	Off
9 - Charge switch	Isolate

Capacitor is now ready to fire.

APPENDIX C

TRACER ANALYSIS THEORY

If gold 198 is produced at a rate P, if the activity is A, and if the decay constant is λ, then

$$\frac{dA}{dt} = \lambda(P - A) = \lambda P - \lambda A \tag{C-1}$$

Assuming a constant flux a solution to equation (C-1) is:

$$A = P(1 - e^{-\lambda t_e}) = A_s(1 - e^{-\lambda t_e}) \tag{C-2}$$

where t_e = time of exposure

A_s = Saturation activity; i.e., the activity approached for an irradiation for a long time compared to the mean lifetime $1/\lambda$.

If the activity at the end of irradiation is A_o and a count is made on the detector between time t_1 and t_2 measured from the end of the exposure, the number of counts C during time $t_2 - t_1$ is

$$C = F\varepsilon \int_{t_1}^{t_2} A_o e^{-\lambda t} dt + B$$
$$= F\varepsilon A_o/\lambda (e^{-\lambda t_1} - e^{-\lambda t_2}) + B \tag{C-3}$$

where F = geometry correction for counter

ε = counter efficiency

B = background counts occurring between t_1 and t_2

Rewriting equation (C-3)

$$C = F\varepsilon \frac{A_o}{\lambda} e^{-\lambda t_1}\{1 - e^{-\lambda(t_2 - t_1)}\} + B$$
$$= F\varepsilon \frac{A_o}{\lambda} e^{-t\omega}(1 - e^{-\lambda t_c}) + B \tag{C-4}$$

where C = number of counts for time interval t_c

t_c = counting time

B = background counts for time interval t_c

t_w = waiting period measured from time of exposure

Combining equations (C-2) and (C-4) and using the fact that

$$A = A_o e^{-\lambda t_w} \tag{C-5}$$

we have:

$$A_s = \frac{\lambda (C - B)}{F\varepsilon (1 - e^{-\lambda t_e})(e^{-\lambda t_w})(1 - e^{-\lambda t_c})}$$

For our case:

$$A_{sc} = \frac{\lambda_c (C_c - B_c)}{F_c \varepsilon_c (1 - e^{-\lambda_c t_{ec}})(e^{-\lambda_c t_{wc}})(1 - e^{-\lambda_c t_{cc}})} \tag{C-6}$$

$$A_{ss} = \frac{\lambda_s (C_s - B_s)}{F_s \varepsilon_s (1 - e^{-\lambda_s t_{es}})(e^{-\lambda_s t_{ws}})(1 - e^{-\lambda_s t_{cs}})} \tag{C-7}$$

where A_{sc} = saturation activity of control sample

A_{ss} = saturation activity of sample disk

Dividing equation (C-6) by (C-7) we obtain:

$$\frac{A_{sc}}{A_{ss}} = \frac{\dfrac{\lambda_c (C_c - B_c)}{F_c \varepsilon_c (1 - e^{-\lambda_c t_{ec}})(e^{-\lambda_c t_{wc}})(1 - e^{-\lambda_c t_{cc}})}}{\dfrac{\lambda_s (C_s - B_s)}{F_s \varepsilon_s (1 - e^{-\lambda_s t_{es}})(e^{-\lambda_s t_{ws}})(1 - e^{-\lambda_s t_{cs}})}} \tag{C-8}$$

But, $F_c = F_s$

$\varepsilon_c = \varepsilon_s$

$B_c = B_s = B$

$\lambda_c = \lambda_s$

$t_{cc} = t_{cs}$

$t_{ec} = t_{es}$

Therefore:

$$\frac{A_{sc}}{A_{ss}} \quad \frac{(C_c - B)}{(C_s - B)} \quad \frac{e^{-\lambda t_{ws}}}{e^{-\lambda t_{wc}}} \tag{C-9}$$

The saturation activity for a steady neutron flux for a thin foil is given by (6):

$$A_s = N_t \int_0^\infty \sigma_a(E)\, \phi(E)\, dE \tag{C-10}$$

where N_t = number of target atoms = $\rho \frac{N_a}{A.W.} V$

and ρ = density, σ = microscopic cross section for absorption, A.W. = atomic weight, V = volume, ϕ = flux, N_a = Avagadro's number

However since ρV is the mass of the target atoms we obtain:

$$N_t = \frac{V \rho N_a}{A.W.} = \frac{m N_a}{A.W.} \tag{C-11}$$

where m = mass of gold

Substituting equation (C-11) into equation (C-10) we obtain:

$$A_s = \frac{m N_a}{A.W.} \sigma \phi \tag{C-12}$$

or from equation (C-2):

$$A = (1 - e^{-\lambda t_e}) \frac{m N_a}{A.W.} \sigma \phi \tag{C-13}$$

Now by forming the ratio of the activities of the control sample and unknown sample we obtain:

$$\frac{A_{sc}}{A_{ss}} = \frac{A_c}{A_s} = \frac{N_{tc}}{N_{ts}} \cdot \frac{\sigma_c \phi}{\sigma_s \phi} = \frac{N_{tc}}{N_{ts}} \tag{C-14}$$

or since $\sigma_s = \sigma_c$ and $\phi_c = \phi_s$

$$N_{ts} = \frac{N_{tc} A_s}{A_c} \qquad \text{(C-15)}$$

Putting this equation in terms of the known and unknown masses:

$$\frac{m_s N_a}{A_s w} \qquad \left[\frac{m_c N_a}{A_c w_c}\right]\left[\frac{A_s}{A_c}\right] \qquad \text{(C-16)}$$

Using equation (C-9) and substituting for A_s/A_c we obtain:

$$m_s = \frac{\left[\quad\right] C^{-\lambda_c t w_c}}{\left[\quad\right] C^{-\lambda_s t w_s}} m_c \qquad \text{(C-17)}$$

APPENDIX D

COUNTING PROCEDURE

1 - Sample	Place on top of crystal
At M-unit	
2 - Mode	Stop 1
At F-unit	
3 - Conversion gain	256
4 - Clock	Set
5 - Fine Gain	20.6
6 - Zero Level	0.0
7 - Threshold	10.2
8 - Corase Gain	8.0
9 - Coincidence	Free
At R-unit	
10 - Analog	Log
11 - Digital	Off
At M-unit	
12 - Counts	Set
13 - Group	1and2
14 - Display	Over Halves
15 - Readout	CRT
16 - Live Time	Set
17 - Experiemnt	PHA
18 - Mode	Analyze
19 - Teletype	On
20 - Readout	Digital

Number of counts in each channel will be printed at end of counting time.

APPENDIX E

PREPARATION OF CONTROL SAMPLES

A small amount of gold foil was torn from a larger sheet and carefully weighed on an experimental balance. After the foil was weighed, it was placed on a piece of standard household aluminum foil which had been sprayed with a coat of lacquer and was still wet. The mass of gold foil adhered to the lacquered surface. After the surface dried, another coat of lacquer was applied to secure the foil in place. A control disk 0.73 inches in diameter containing this known mass of gold was then cut and used as a gold control sample during irradiation and counting.

The aluminum control samples were simply cut from a piece of lacquered aluminum foil and included in each group during irradiation.

INITIAL DISTRIBUTION LIST

		No. Copies
1.	Defense Documentation Center Cameron Station Alexandria, Virginia 22314	20
2.	Library Naval Postgraduate School Monterey, California 93940	2
3.	Commander, Naval Air Systems Command Department of the Navy Washington, D. C. 20360	1
4.	Professor D. C. Wooten Department of Aeronautics Naval Postgraduate School Monterey, California 93940	5
5.	Chairman, Department of Aeronautics Naval Postgraduate School Monterey, California 93940	1
6.	Professor A. E. Fuhs Department of Aeronautics Naval Postgraduate School Monterey, California 93940	1
7.	Michael J. Smith, Ens., USN P. O. Box 206 Beaufort, N. C. 28516	3
8.	Superintendent U. S. Naval Academy Annapolis, Maryland 21402	1
9.	Head, Engineering Department U. S. Naval Academy Annapolis, Maryland 21402	1
10.	Dr. E. S. Lamar (Code 03C) Chief Scientist Naval Air Systems Command Navy Department Washington, D. C. 20360	1
11.	Commander Naval Ordnance Systems Command Department of the Navy Washington, D. C. 20360	1

12. Office of Naval Research 1
Navy Department
Washington, D. C. 20360

13. Mr. E. C. Cooper 1
Advanced Systems Concepts Div.
Research and Technology (Code 303A)
Naval Air Systems Command
Navy Department
Washington, D. C. 20360

14. Mr. I. Silver 1
Propulsion Administrator (Code 330)
Research and Technology
Naval Air Systems Command
Navy Department
Washington, D. C. 20360

15. Office of Naval Research 1
Physical Sciences Division, (Code 420)
Navy Department
Washington, D. C. 20360

16. Office of Naval Research 1
(Attn: R. D. Cooper, Code 438)
Math Sciences Division
Office of Naval Research
Navy Department
Washington, D. C. 20360

17. Office of Naval Research 1
Air Programs Office
Navy Department
Washington, D. C. 20360

DOCUMENT CONTROL DATA - R&D

(Security classification of title, body of abstract and indexing annotation must be entered when the overall report is classified)

1. ORIGINATING ACTIVITY (Corporate author)	2a. REPORT SECURITY CLASSIFICATION
Naval Postgraduate School Monterey, California 93940	Unclassified
	2b. GROUP

3. REPORT TITLE

AN EXPERIMENTAL INVESTIGATION OF THE EFFECTS OF ENVIRONMENTAL PRESSURE ON THE EXHAUST OF A COAXIAL PLASMA GUN

4. DESCRIPTIVE NOTES (Type of report and inclusive dates)

Thesis

5. AUTHOR(S) (Last name, first name, initial)

SMITH, Michael J.

6. REPORT DATE	7a. TOTAL NO. OF PAGES	7b. NO. OF REFS
March 1968	91	12

8a. CONTRACT OR GRANT NO.	9a. ORIGINATOR'S REPORT NUMBER(S)
b. PROJECT NO.	
c.	9b. OTHER REPORT NO(S) (Any other numbers that may be assigned this report)
d.	

10. AVAILABILITY/LIMITATION NOTICES

~~This document is subject to special export controls and each transmittal to foreign governments or foreign nationals may be made only with prior approval of the Naval Postgraduate School~~

11. SUPPLEMENTARY NOTES	12. SPONSORING MILITARY ACTIVITY
	Naval Postgraduate School Monterey, California 93940

13. ABSTRACT

A coaxial plasma accelerator system was restored to working order and procedures for operating the system were established. Gold was used as the working material and was mounted as a thin circular foil between coaxial electrodes, ionized, and accelerated by discharging a high energy capacitor across the electrodes.

Downstream of the electrodes, part of the gold was collected on a cylindrical collector sheet of aluminum foil. This sheet surrounded the outer electrode and extended 16 inches above the muzzle. A radioisotope tracer technique was then used to determine the mass of deposited gold on sample disks cut from selected portions of the collector sheet. It was found that only a very small percentage of the total mass was collected and that the pressure effects, in the range from 5×10^{-5} mm Hg to 50×10^{-3} mm Hg, were such that an increase in exhaust pressure caused an increase in the mass of gold collected on the sheet; however, pressure effects on the distribution of this mass were negligible.

DD FORM 1 JAN 64 1473

14 KEY WORDS	LINK A		LINK B		LINK C	
	ROLE	WT	ROLE	WT	ROLE	WT
Coaxial Plasma Accelerator						
Radioisotope Tracing Technique						
Magnetohydrodynamics